Innate signaling promotes formation of regulatory nitric oxide-producing dendritic cells limiting T-cell expansion in experimental autoimmune myocarditis

Kania, Gabriela ; Siegert, Stefanie ; Behnke, Silvia ; Prados-Rosales, Rafael ; Casadevall, Arturo ; Lüscher, Thomas F ; Luther, Sanjiv A ; Kopf, Manfred ; Eriksson, Urs ; Blyszczuk, Przemyslaw

Abstract: BACKGROUND: Activation of innate pattern-recognition receptors promotes CD4+ T-cell-mediated autoimmune myocarditis and subsequent inflammatory cardiomyopathy. Mechanisms that counterregulate exaggerated heart-specific autoimmunity are poorly understood. METHODS AND RESULTS: Experimental autoimmune myocarditis was induced in BALB/c mice by immunization with -myosin heavy chain peptide and complete Freund's adjuvant. Together with interferon- , heat-killed Mycobacterium tuberculosis, an essential component of complete Freund's adjuvant, converted CD11b(hi)CD11c(-) monocytes into tumor necrosis factor- - and nitric oxide synthase 2-producing dendritic cells (TipDCs). Heat-killed M. tuberculosis stimulated production of nitric oxide synthase 2 via Toll-like receptor 2-mediated nuclear factor- B activation. TipDCs limited antigen-specific T-cell expansion through nitric oxide synthase 2-dependent nitric oxide production. Moreover, they promoted nitric oxide synthase 2 production in hematopoietic and stromal cells in a paracrine manner. Consequently, nitric oxide synthase 2 production by both radiosensitive hematopoietic and radioresistant stromal cells prevented exacerbation of autoimmune myocarditis in vivo. CONCLUSIONS: Innate Toll-like receptor 2 stimulation promotes formation of regulatory TipDCs, which confine autoreactive T-cell responses in experimental autoimmune myocarditis via nitric oxide. Therefore, activation of innate pattern-recognition receptors is critical not only for disease induction but also for counterregulatory mechanisms, protecting the heart from exaggerated autoimmunity.

DOI: https://doi.org/10.1161/CIRCULATIONAHA.112.000434

DOI: 10.1161/CIRCULATIONAHA.112.000434

Innate Signalling Promotes Formation of Regulatory Nitric Oxide-Producing Dendritic Cells Limiting T Cell Expansion in Experimental Autoimmune Myocarditis

Running title: *Kania et al.; Nitric oxide in EAM*

Gabriela Kania, PhD[1,2]; Stefanie Siegert, PhD[3]; Silvia Behnke, PhD[4]; Rafael Prados-Rosales, PhD[5]; Arturo Casadevall, PhD[5]; Thomas F. Lüscher, MD[1,6]; Sanjiv A. Luther, PhD[3]; Manfred Kopf, PhD[7]; Urs Eriksson, MD[1,2*]; Przemyslaw Blyszczuk, PhD[1,2*]

[1]Cardioimmunology, Cardiovascular Research, Zurich Center for Integrative Human Physiology, University of Zurich, Zurich; [2]Dept of Medicine, GZO - Zurich Regional Health Centre, Wetzikon; [3]Dept of Biochemistry, University of Lausanne, Epalinges; [4]Sophistolab AG, Eglisau, Switzerland; [5]Dept of Microbiology and Immunology, Albert Einstein College of Medicine, New York, NY; [6]Cardiology, Cardiovascular Centre, University Hospital, Zurich; [7]Molecular Biomedicine, Institute of Integrative Biology, ETH Zurich, Zurich, Switzerland

* shared last authorship

Address for Correspondence:

Przemyslaw Blyszczuk, PhD

Cardioimmunology, Cardiovascular Research

Institute of Physiology, University of Zurich

Winterthurerstrasse 190

CH-8057 Zurich, Switzerland

Tel: ++41-44-635-5070

Fax: ++41-44-635-6827

E-mail: przemyslaw.blyszczuk@uzh.ch

Journal Subject Code: Heart failure:[11] Other heart failure

DOI: 10.1161/CIRCULATIONAHA.112.000434

Abstract:

Background—Activation of innate pattern recognition receptors promotes $CD4^+$ T cell-mediated autoimmune myocarditis and subsequent inflammatory cardiomyopathy. Mechanisms, which counter-regulate exaggerated heart-specific autoimmunity are poorly understood.

Methods and Results—Experimental Autoimmune Myocarditis (EAM) was induced in BALB/c mice by immunization with alpha-myosin heavy chain peptide (αMyHC) and complete Freund's adjuvant (CFA). Together with IFN-γ, heat-killed *M. tuberculosis* (Mtb^{hk}), an essential component of CFA, converted $CD11b^{hi}CD11c^-$ monocytes into TNFα- and nitric oxide synthase 2 (NOS2)-producing dendritic cells (TipDCs). Mtb^{hk} stimulated NOS2 production via Toll-like receptor (TLR)2-mediated NF-κB activation. TipDCs limited antigen-specific T cell expansion through NOS2-dependent nitric oxide production. Moreover, TipDCs promoted NOS2 production in hematopoietic and stromal cells in a paracrine manner. Consequently, NOS2 production by both, radiosensitive hematopoietic and radioresistant stromal cells prevented exacerbation of autoimmune myocarditis *in vivo*.

Conclusions—Innate TLR2 stimulation promotes formation of regulatory TipDCs, which confine autoreactive T cell responses in EAM via nitric oxide. Therefore, activation of innate pattern recognition receptors is not only critical for disease induction, but also for counter-regulatory mechanisms, protecting the heart from exaggerated autoimmunity.

Key words: myocarditis, nitric oxide, immunology, autoimmunity

DOI: 10.1161/CIRCULATIONAHA.112.000434

Introduction

Inflammatory dilated cardiomyopathy refers to an end stage heart failure phenotype, which often results from myocarditis. Clinical observations and animal experiments suggest that infection-triggered autoimmunity plays an important role in myocarditis development and its progression to inflammatory dilated cardiomyopathy. Autoimmunity develops as a result of a breakdown in immunological tolerance leading to the activation of self-reactive T lymphocytes. Heart-specific autoimmunity is a consequence of the lack of T cell tolerance to heart-specific alpha-myosin heavy chain (αMyHC) in mice and in humans[1,2]. Activation of pattern recognition receptors on innate immune cells is widely believed to control the development of autoimmunity. Stimulation of Toll-like receptors (TLRs) on antigen presenting cells (APCs) represents an essential step in activation and differentiation of autoreactive, naïve T cells into pathogenic, disease-mediating T helper (Th) cells[3,4].

Commonly used animal models of autoimmune diseases are based on the delivery of self-antigen together with complete Freund's adjuvant (CFA) containing heat-killed *M. tuberculosis* (*Mtb*^{hk}) as its active component. In experimental autoimmune myocarditis (EAM), administration of alpha-myosin heavy chain (α-MyHC) peptide and CFA into BALB/c mice results in self-limiting, CD4^{+} Th cell-mediated heart-specific inflammation[5-9].

IFN-γ-producing Th1 cells represent a major subset of CD4+ T cells infiltrating the myocardium in EAM. However, the role of Th1 cells and IFN-γ in pathogenesis of heart-specific autoimmunity is unclear. Mice lacking IFN-γ or its receptor are highly susceptible to EAM induced with α-MyHC/CFA[10-12]. In contrast, in transgenic mouse model of spontaneous heart-specific autoimmunity, IFN-γ deficiency results in reduced myocarditis[2].

Nitric oxide synthase (NOS)2 represents an inducible isoform of NOS, which is absent in

healthy myocardium, but has been clearly associated with tissue damage in patients with ischemic and nonischemic heart failures. In animal models, NOS2-producing cells have been reported to infiltrate the myocardium of α-MyHC/CFA immunized mice[10] and upon infection with Coxsackievirus[13] or *T. cruzi*[14]. In EAM, NOS2 production entirely depends on IFN-γ[10]. NOS2-dependent nitric oxide has been shown to functionally eliminate heart-specific infections[15,16], however its definitive role in the regulation of infection triggered heart-specific autoimmunity remains elusive.

NOS2 is produced by various cell types including macrophages, activated monocytes, stromal fibroblastic and endothelial cells. TNFα- and iNOS-producing dendritic cells (TipDCs) represent another cell subset, which is capable to produce nitric oxide[17,18]. TipDCs originate from monocytes and therefore belong to a subset of monocyte-derived DCs. In contrast to conventional DCs, monocyte-derived DCs readily accumulate during infections and inflammation[19]. Both, conventional and monocyte-derived DCs express CD11c, MHC class II and are effective antigen presenters, but they can be distinguished by CD64 antigen expression[19]. Monocyte-derived TipDCs were reported to mediate the innate immune defence against bacterial infections[17]. Their role in the regulation of adaptive immune responses remains unclear.

Here, we show how TLR2 activation together with IFN-γ signalling converts monocytes into TipDCs, which limit T cell expansion and EAM development through nitric oxide. Our study reveals a novel principle of how cooperation of innate and adaptive mechanisms confines autoreactive heart-specific T cell responses.

Materials and Methods

Mice Balb/C mice (n=86) and *Rag2*$^{-/-}$ (n=39), *Ifng*$^{-/-}$ (n=15), *Ifngr1*$^{-/-}$ (n=9), *Myd88*$^{-/-}$ (n=4),

Nos2$^{-/-}$ (n=44) and DO11.10-*tg* (n=20) mice on Balb/C background were described previously[7,10,11,20,21]. *Rag2*$^{-/-}$*Ifngr1*$^{-/-}$ mice (n=15) were created by crossing *Rag2*$^{-/-}$ and *Ifngr1*$^{-/-}$ mice. In the respective *in vitro* experiments, cells were isolated from C57BL/6 mice (n=8) and *Tlr2*$^{-/-}$ (n=12), CD45.1-*tg*, (n=4) OT-II-*tg* (n=8) and *Nos2*$^{-/-}$ (n=4) mice on C57BL/6 background (all originally Jackson Laboratory). Animal experiments were performed in accordance with the Swiss federal law and were approved by the local authorities.

EAM induction

To induce EAM mice were injected subcutaneously with 150 µg of α-MyHC (Ac-RSLKLMATLFSTYASADR-OH; Caslo) peptide emulsified 1:1 with Complete Freund's Adjuvant (CFA, Difco) on days 0 and 7. In the respective experiments mice were injected with 150 µg of α-MyHC peptide emulsified 1:1 with Incomplete Freund's Adjuvant (IFA, Difco).

Chimeric mice

Bone marrow chimeras: 6-8 week old mice were lethally irradiated with two doses of 6.5 Gy as described and transplanted with total of 2x10^7 crude donor bone marrow and used 6 weeks after bone marrow reconstitution. *Rag2*$^{-/-}$ chimeras: 6-8 week old *Rag2*$^{-/-}$ or *Rag2*$^{-/-}$*Ifngr1*$^{-/-}$ mice received total of 10^7 naïve splenocytes and were used 3 weeks after cell transfer.

Histopathology and Immunocytochemistry

Tissues were fixed in formalin or HOPE (DCS-Diagnostic) and embedded in paraffin. Antigen retrieval procedure was performed using ER2 buffer (Leica) and sections were stained with rat anti-mouse CD45 (BD Bioscience), rabbit anti-mouse CD3 (Neomarkers), rabbit anti-NOS2 (Millipore) and rabbit anti-rat IgG (Abcam) antibodies and the Bond Polymer Refine Detection kit using the BOND-MAX system (both Leica). Immunopositive cells were quantified using analySIS FIVE software (Olympus). For NF-κB p65 translocation, cells were stimulated for 30

min, fixed with 4% paraformaldehyede, permeabilized with 0.5% saponin (both Sigma) and stained with rabbit anti-NF-κB p65 (Abcam) and AlexaFluor488 anti-rabbit IgG (Invitrogen).

[3H]-thymidine proliferation assay

$CD4^+$ T cell magnetic beads (Miltenyi) were used to purify $CD4^+$ T cells. CD4-negative population was used as APCs. A total of $5x10^4$ $CD4^+$ T cells co-cultured with 10^5 irradiated (25 Gy) syngeneic APCs were re-stimulated for 48h in the presence of serial dilutions of the α-MyHC peptide. Proliferation was assessed by measuring [3H]-thymidine incorporation during the last 8-16 hours.

Flow cytometry and FACS

Single cell suspensions were prepared from digested hearts treated with 0.2 mg/mL Liberase (Roche) for 45 min, lymph nodes treated with 3 mg/mL Collagenase D and 1 mg/mL DNAse (both Sigma) for 30 min and cultured cells using 70µm and 40µm cell strainers. Cells were incubated with the appropriate combination of fluorochrome-conjugated antibodies (available in the supplemental material). Samples were analysed with the FACSCanto analyser (BD Bioscience) and FlowJo software (Tree Star). Proliferation index (number of divisions of dividing cells) of CFSE-labeled cells was computed using FlowJo software. In the respective experiments, cells were sorted with FACSAria III (BD Bioscience).

ELISA

Protein levels in supernatants were measured using mouse NOS2 (EIAab) and mouse TNFα (BD Bioscience) ELISA kits.

Quantitative RT-PCR

RNA was isolated with RNeasy Plus Kits (Qiagen) and cDNA was amplified using the Power SYBR Green PCR Master Mix (Applied Biosystems). *Nos2* was detected using 5'-

cagctgggctgtacaaacctt-3'and 5'-tgaatgtgatgtttgcttcgg-3' oligonucleotides. *Gapdh* levels were used for normalization.

Nitric oxide measurement

Concentrations of nitrite ($NO2^-$) levels reflecting NO production were measured using the Griess Reagent System (Promega).

Statistics

Normally distributed data were analysed by unpaired, two-tailed Student's *t*-test and by one-way ANOVA followed by Bonferroni post-hoc test. All analyses were computed using GraphPad Prism 5 software. Differences were considered as statistically significant for $p<0.05$ (for multiple comparisons adjusted with the Bonferroni correction).

Cell cultures

Description of cell cultures is available in the supplemental material

Results

IFN-γ signalling on non-lymphocytes limits T cell expansion in EAM

Previous studies reported that IFN-γ- and IFN-γR-deficient mice immunized with α-MyHC/CFA developed exacerbated myocarditis, post-inflammatory fibrosis and cardiac dysfunction[10-12] indicating that IFN-γ priming, expansion, and/or differentiation of Th cells in EAM. Indeed, in hearts of IFN-γ deficient (*Ifng*$^{-/-}$) mice we observed an increased number of $CD45^+$ cells (**Fig. 1A**) and $CD3^+$ T lymphocytes (**Fig. 1B**), which peaked at day 16 of EAM. Restimulation of wild-type or *Ifng*$^{-/-}$ $CD4^+$ T splenocytes with α-MyHC peptide in the presence of wild-type or *Ifngr1*$^{-/-}$ APCs showed that IFN-γ production by T cells suppressed their proliferation indirectly through IFN-γR signalling in APCs (**Fig 1C,D**). These data suggest that exaggerated

autoimmunity of *Ifng*$^{-/-}$ mice is not due to intrinsic CD4^{+} T cell hyperproliferation.

To verify this finding *in vivo*, we used a model of *Rag2*$^{-/-}$ mice (lacking T and B cells) injected with donor naïve splenocytes, which restored T and B subsets in *Rag2*$^{-/-}$ mice, but did not contribute to other hematopoietic compartments (**Supplemental Fig. 1**). Accordingly, we generated mixed chimera by adoptive transfer of a mixture of CD45.1^{+}wild-type and CD45.2^{+}*Ifngr1*$^{-/-}$ splenocytes into *Rag2*$^{-/-}$ mice 3 weeks prior to α-MyHC/CFA immunization. In these mice all CD3^{+}CD4^{+} T cells derived from donor splenocytes. At day 16 of EAM, we observed unchanged CD45.1^{+}:CD45.2^{+} T cell ratio in the spleen and inflamed hearts (**Fig. 1E**) indicating comparable expansion of autoimmune α-MyHC-specific wild-type and *Ifngr1*$^{-/-}$ CD4^{+} T cells. Moreover, *Rag2*$^{-/-}$ mice reconstituted with either wild-type or *Ifngr1*$^{-/-}$ cells showed comparable cardiac infiltrations with inflammatory CD45^{+} (**Fig. 1F**) and CD3^{+} (**Fig. 1G**) cells after α-MyHC/CFA immunization. In contrast, increased myocarditis was observed in *Rag2*$^{-/-}$ *Ifngr1*$^{-/-}$ relative to *Rag2*$^{-/-}$ mice reconstituted with wild-type splenocytes prior immunization (**Fig. 1H,I**). Thus, our results unequivocally demonstrate that IFN-γR-signalling in the non-lymphocytic compartment controls T cell expansion in α-MyHC/CFA immunized mice.

Heat-killed *M. tuberculosis* activates TLR2 to induce IFN-γ-dependent nitric oxide production

Next, we studied how IFN-γ regulates T cell expansion in the immune system. DO11.10-*tg* and OT-II-*tg* mice express transgenic T cell receptor recognizing a peptide from chicken ovalbumin (OVA). We isolated CD4^{+} T cells from DO11.10-*tg* mice and injected them into *Rag2*$^{-/-}$ or *Rag2*$^{-/-}$*Ifngr1*$^{-/-}$ mice treated with IFA or CFA with or without OVA peptide. In agreement with the data above, DO11.10-*tg* CD4^{+} T cells showed much greater antigen-specific proliferation in the spleen of *Rag2*$^{-/-}$*Ifngr1*$^{-/-}$ compared to *Rag2*$^{-/-}$ mice (**Fig. 2A**). Notably, even antigen

unspecific proliferation was enhanced in *Rag2*$^{-/-}$*Ifngr1*$^{-/-}$ mice treated with CFA.

CFA, in contrast to IFA, contains heat-killed *Mycobacterium tuberculosis* (*Mtb*^{hk}). To better understand the role of *Mtb*^{hk} in T cell response, we isolated splenocytes from *Rag2*$^{-/-}$ and *Rag2*$^{-/-}$ *Ifngr1*$^{-/-}$ mice and co-cultured them with CD4^{+} T cells from DO11.10-*tg* mouse in the presence or absence of *Mtb*^{hk} and OVA peptide. Interestingly, *Mtb*^{hk} potently inhibited CD4^{+} T cell proliferation, which was dependent on intact IFN-γR-signalling in APCs (**Fig. 2B**). IFN-γ is known to regulate several metabolic pathways including arginine metabolism and tryptophan catabolism controlling T cell responses. L-NAME, a competitive inhibitor of all NOS isoforms, greatly enhanced CD4^{+} T cell proliferation in the presence of *Rag2*$^{-/-}$ (**Fig. 2C**) but not of *Rag2*$^{-/-}$*Ifngr1*$^{-/-}$ (**Fig. 2E**) splenic APCs, while no differences were observed by inhibition of arginase-1 and indoleamine 2,3-dioxygenase using the inhibitors Nor-NOHA and 1-methyl-tryptophan, respectively. Accordingly, co-cultures of CD4^{+} T cells and IFN-γR-competent splenocytes in the presence of L-NAME, but not Nor-NOHA or 1-methyl-tryptophan, revealed reduced nitrate levels reflecting reduced nitric oxide production (**Fig. 2D,F**). These results strongly suggest that T cell proliferation is suppressed via IFN-γR induced nitric oxide production by splenocytes. Consistently, we observed elevated nitrate levels in supernatants of proliferating CD4^{+} T cells in the presence of IFN-γR-sufficient, but not IFN-γR-deficient splenocytes, (**Fig. 2G**). Importantly, while signalling from proliferating T cells was sufficient to induce nitric oxide production, the addition of *Mtb*^{hk} greatly enhanced it.

Furthermore, bacterial lipoproteins such as Pam3CSK4 and FSL-1 potently inhibited CD4^{+} T cell proliferation and boosted nitric oxide production. In contrast, microbial nucleic acids such as Poly(I:C) or ODN1826 enhanced CD4^{+} T cell proliferation and reduced nitrate levels (**Supplemental Fig. 2**).

Culture of *Rag2*$^{-/-}$ and *Rag2*$^{-/-}$*Ifngr1*$^{-/-}$ splenocytes in the absence of T cells showed that stimulation with both IFN-γ and *Mtb*^{hk} was essential for up-regulation of *Nos2* transcripts (**Fig. 2H**), detectable NOS2 protein (**Fig. 2I**) and elevated nitrate levels (**Fig. 2J**) in the supernatant. Taken together these data suggest that stimulation of myeloid cells with IFN-γ together with *Mtb*^{hk} restrains CD4^{+} T cell proliferation via nitric oxide production.

M. tuberculosis is recognized by immune cells primarily via TLR2, which induces the NF-κB signalling pathway. Using NF-κB specific reporter cells, we showed that *Mtb*^{hk}, as well as native membrane vesicles (MV) produced by *M. tuberculosis* (*Mtb* MV) used TLR2 to activate NF-κB (**Fig. 3A,B**). As expected, TNFα activated the NF-κB pathway TLR2 independently (**Fig. 3A,B**). *Mtb*^{hk} or *Mtb* MV treatment of macrophages also induced nuclear translocation of NF-κB p65 (**Fig. 3C**). Furthermore, macrophages treated with *Mtb*^{hk} in the presence of IFN-γ showed TLR2-dependent nitric oxide (**Fig. 3D**) and TNFα (**Fig. 3E**) production.

Next, we pre-treated *Rag2*$^{-/-}$ splenocytes with the irreversible NF-κB inhibitor Bay 11-7082 (Bay) and stimulated them with *Mtb*^{hk} and IFN-γ. Bay completely prevented *Nos2* up-regulation (**Fig. 3F**) and nitrate oxide production (**Fig. 3G**). Furthermore, *Rag2*$^{-/-}$ splenocytes pretreated with Bay were unable to inhibit T cell proliferation, consistent with the lack of nitric oxide production (**Fig. 3H,I**). Our data demonstrate that *Mtb*^{hk} requires TLR2 to induce NF-κB-dependent nitric oxide production.

M. tuberculosis antigens in cooperation with IFN-γ convert monocytes into nitric oxide-producing dendritic cells

So far, it was unclear which cells produced nitric oxide in response to IFN-γ and *Mtb*^{hk} stimulation. Analysis of intracellular NOS2 in *Rag2*$^{-/-}$ splenocytes pointed to CD11b^{hi}CD11c^{+}

cells as major nitric oxide producers (**Fig. 4A**). CD11b^{hi}CD11c^{+} cells, however, are present in low numbers only in spleens and LNs of naïve mice (**Fig. 4B**). We found that they developed readily from CD11b^{hi}CD11c^{-} monocytes, when exposed to *Mtb*^{hk} or IFN-γ (**Fig. 4C**). In fact, stimulation of sorted CD11b^{hi}CD11c^{-} monocytes with IFN-γ or *Mtb*^{hk} induced expression of CD11c and CD64, but co-stimulation with IFN-γ and *Mtb*^{hk} or TNFα was required to boost NOS2 (**Fig. 4C**) and nitric oxide production (**Fig. 4D**). Notably, IFN-γ and *Mtb*^{hk} exerted distinct activities on CD11b^{hi}CD11c^{-} monocytes up-regulating MHC class II (**Fig. 4C**) and TNFα production respectively (**Fig. 4E**). Our data showed that, *Mtb*^{hk} and IFN-γ converted CD11b^{hi}CD11c^{-} monocytes into TNFα- and NOS2-producing DCs. This subset of DCs has been previously described and termed TipDCs[17].

Our findings showed that *Mtb*^{hk}-stimulated TipDCs massively produce TNFα, which potentially could boost locally NOS2 production. As shown above, *Mtb*^{hk} is specifically recognized by TLR2, and therefore stimulation with IFN-γ and *Mtb*^{hk} resulted in impaired NOS2 production in CD11b^{hi}CD11c^{-} *Tlr2*$^{-/-}$ cells (**Fig. 4F**). Instead, co-culture with wild-type TipDCs boosted NOS2 production in *Tlr2*$^{-/-}$ cells (**Fig. 4G**). This result clearly indicates that *Mtb*^{hk}-activated TipDCs contribute to positive regulation of NOS2 in neighbouring cells.

DCs are specialized in capturing, processing and presenting of antigens to T cells. We found that in contrast to CD11b^{hi}CD11c^{-} monocytes, naïve and *Mtb*^{hk}/IFN-γ-activated CD11b^{hi}CD11c^{+} DCs effectively induce antigen-specific T cell proliferation (**Fig. 5A**). This result indicates that monocytes converting into DC phenotype acquire APC properties.
So far, definitive evidence that nitric oxide produced by TipDCs limits T cell expansion is lacking. CD11b^{hi}CD11c^{-} cells with a disrupted *Ifngr1 MyD88* or *Tlr2* gene stimulated with IFN-γ and *Mtb*^{hk} showed impaired *Nos2* expression (**Fig. 5B,F**) and failed to produce nitric oxide (**Fig.**

5C,G) confirming that IFN-γR-signaling and *Mtb*^{hk}-induced TLR2/MyD88 signalling was crucial for development of nitric oxide-producing TipDCs. Next, we co-cultured OVA-reactive CD4$^+$ T cells with conventional DCs in the presence of CD11b^{hi}CD11c$^-$ cells, OVA peptide and *Mtb*^{hk}. We observed uncontrolled T cell proliferation (**Fig. 5D,H**) and reduced nitric oxide (**Fig. 5E,I**) in the presence of *Nos2*$^{-/-}$, *Ifngr1*$^{-/-}$, *MyD88*$^{-/-}$ or *Tlr2*$^{-/-}$ monocyte-derived DCs. This result clearly demonstrates that NOS2 production defines the regulatory role of monocyte-derived DCs.

TipDCs promote nitric oxide production in stromal fibroblasts

Stromal cells represent another important source of NOS2-derived nitric oxide. We used the nitric oxide-producing pLN2 cell line established from LN fibroblasts to address whether *M. tuberculosis* antigens affect nitric oxide production in this cell type. However, stimulation with Pam3CSK4, *Mtb*^{hk} or *Mtb* MV failed to induce NF-κB p65 nuclear translocation on pLN2 cells, probably due to insufficient TLR2 expression (**Fig. 6A,B**). Instead, TNFα induced translocation of NF-kB p65 into nucleus (**Fig. 6A,B**) and in cooperation with IFN-γ promoted *Nos2* expression and nitric oxide production in these fibroblasts (**Fig. 6C,D**). Accordingly, addition of *Mtb*^{hk} or *Mtb* MV to co-cultures of pLN2 with conventional DCs and OT-II-*tg* CD4$^+$ T cells failed to affect antigen-specific T cell proliferation and nitric oxide levels (**Fig. 6E,F**). Thus, these results demonstrate that TLR2 is required for *Mtb*^{hk}-induced nitric oxide production not only in myeloid, but also in stromal cells.

We demonstrated that *Mtb*^{hk} induced production of cytokines, such as TNFα, which could stimulate NOS2 production in monocyte-derived DCs and in pLN2 cells. To analyze, whether TipDCs activated with *Mtb*^{hk} can stimulate NOS2 production in stromal cells, we sorted CD11b^{hi}CD11c$^-$ from *Nos2*$^{-/-}$ splenocytes and co-cultured them with pLN2 cells in the presence

or absence of *Mtb*^{hk}. Indeed, addition of *Mtb*^{hk} induced nitric oxide levels in co-cultures (**Fig. 6G**). Giving that pLN2 cell fail to respond to *Mtb*^{hk}, these results indicate that *Mtb*^{hk}-activated TipDCs can induce nitric oxide production in stromal cells.

Nitric oxide from TipDCs or stromal cells limits EAM progression

So far, our data demonstrated that *Mtb*^{hk} induced NOS2 and nitric oxide production *in vitro*. To analyze its role in EAM development, we subcutaneously injected mice with α-MyHC/CFA into the right groin and with α-MyHC/IFA into the left groin and analyzed 5 days later inguinal lymph nodes (iLNs, **Fig. 7A**). At the side of α-MyHC/CFA injection, iLNs were enlarged and contained more NOS2-producing cells (**Fig. 7B**). Furthermore, CFA-primed iLNs were infiltrated by higher number of CD11b^{hi}CD11c^{+} cells (**Fig. 7C**), which showed enhanced NOS2 levels (**Fig. 7D**). Instead, stromal cells from the CFA- and IFA-primed iLNs showed comparable NOS2 production (**Fig. 7E**). These results suggest that in the EAM model, *Mtb*^{hk} promotes formation of TipDCs at the site of antigen delivery.

To address a direct role of NOS2 in EAM, we immunized BALB/c and *Nos2*$^{-/-}$ mice with α-MyHC/CFA. We observed enhanced myocarditis (**Fig. 8A,B**) and an increased number of infiltrating CD45^{+} cells (**Fig. 8C**) and CD3^{+} T lymphocytes (**Fig. 8D**) in hearts of *Nos2*$^{-/-}$ mice at day 16 of EAM. We found that, both CD11b^{hi}CD11c^{-} monocytes and CD11b^{hi}CD11c^{+} monocyte-derived DCs heavily infiltrate the myocardium in EAM at this time point. As expected, NOS2 was mainly identified in the CD11b^{hi}CD11c^{+} population that also expressed MHC class II and CD64 (**Fig. 8E**) indicating a TipDC phenotype. Furthermore, restimulation of wild-type and *Nos2*$^{-/-}$ CD4^{+} T cells with α-MyHC peptide presented by wild-type or *Nos2*$^{-/-}$ APCs showed that absence of NOS2 in APCs, but not in CD4^{+} T cells, resulted in enhanced α-MyHC-specific T cell proliferation (**Supplemental Fig. 3**).

To verify that nitric oxide produced by inflammatory TipDCs prevented uncontrolled myocarditis, we generated criss-cross bone marrow chimeras by injection of the whole bone marrow from wild-type or *Nos2*$^{-/-}$ mice to lethally irradiated wild-type and *Nos2*$^{-/-}$ recipients. 6 weeks later, we immunized the bone marrow chimeric mice with α-MyHC/CFA to induce EAM. Interestingly, we found elevated numbers of infiltrating CD45^{+} cells (**Fig. 8F**) and CD3^{+} T lymphocytes (**Fig. 8G**) only in *Nos2*$^{-/-}$->*Nos2*$^{-/-}$ chimeras suggesting that nitric oxide production by either radiosensitive hematopoietic cells or by radioresistant non-hematopoietic stromal cells was sufficient to prevent exacerbated myocarditis. Indeed, immunohistochemistry of NOS2 on heart tissue sections from the bone marrow chimeras showed NOS2-positive cells in both hematopoietic (wild-type->*Nos2*$^{-/-}$) and non-hematopoietic compartments (*Nos2*$^{-/-}$->wild-type, **Fig. 8H**). As illustrated above, TipDCs represent major NOS2 producers in hematopoietic inflammatory fraction in EAM. Heart tissue analysis of *Nos2*$^{-/-}$->wild-type chimeras showed that NOS2 was expressed by gp38-positive fibroblasts in the inflamed heart (**Supplemental Fig. 4**). Importantly, NOS2-producing radioresistant stromal cells were only found in the inflamed areas indicating local induction, and NOS2 was undetectable in healthy hearts.

Discussion

In myocarditis, IFN-γ-producing Th1 cells infiltrate the myocardium, but the role of IFN-γ remains unclear. IFN-γ is a proinflammatory cytokine, which when overexpressed induces chronic myocarditis[22]. Furthermore, in transgenic model of spontaneous autoimmune myocarditis, IFN-γ was recognized to promote inflammation[2]. On the other hand, IFN-γ clearly attenuates myocarditis induced with α-MyHC/CFA[10-12] or triggered by viral[23] or parasitic[24] infections. Our data showing increased EAM susceptibility of *Rag2*$^{-/-}$*Ifngr1*$^{-/-}$ chimeric mice

reconstituted with wild-type lymphocytes clearly demonstrated that lack of IFN-γ receptor on non-T cells is responsible for exacerbated T cell expansion and myocarditis in the α-MyHC/CFA model. We identified the well-known IFN-γ-dependent nitric oxide production as the key mechanism limiting autoreactive T cell proliferation in EAM.

Effective NOS2-dependent nitric oxide production requires co-activation of the NF-κB pathway with TLR agonists or pro-inflammatory cytokines, such as TNFα. Activated T cells produce both co-signals (IFN-γ, and TNFα) required for *Nos2* up-regulation. Here, we showed that in addition to T cells, direct innate signalling on myeloid cells remarkably contributes to nitric oxide production. Our data demonstrate that *M. tuberculosis* antigens promoted conversion of $CD11b^{hi}CD11c^{-}$ monocytes into nitric oxide-producing TipDCs. Importantly, TipDCs represent a subset of monocyte-derived DCs, which corresponds to classically activated macrophages and is distinct from conventional DCs[19,25]. In line with previous findings[19,25], we showed that TipDCs massively accumulate during inflammation. A previous report pointed to a proinflammatory role of monocyte-derived DCs in autoimmunity[26]. Indeed, our data show that monocyte-derived DCs express MHC class II and therefore can engage and also potentially expand autoreactive $CD4^{+}$ T cells. Importantly, our data clearly show that nitric oxide produced by TipDCs efficiently suppresses T cell expansion. Therefore, it is important to distinguish TipDCs from other NOS2-negative monocyte-derived DCs because of the opposing effects of these two DC subsets on T cell proliferation. Although the ultimate role of monocyte-derived DCs and TipDCs in autoimmunity has not been fully elucidated yet, our data clearly demonstrate that NOS2 production defines their regulatory function.

Subcutaneous delivery of self-peptides together with CFA represents the most common immunization procedure in rodent models of autoimmune diseases. The presence of Mtb^{hk} in

CFA is critical for the induction of pathogenic T cell response in these models[3]. The innate immune response apparently plays a dual role in regulating adaptive autoimmunity. On one hand, it promotes development of pathogenic Th cells and inflammation. On the other hand, together with IFN-γ, it prevents uncontrolled expansion of activated T cells.

Experiments with bone-marrow chimeras showed that in EAM both hematopoietic and stromal cells produced functional NOS2. We showed that *Mtb*^{hk}-activated TipDCs promote nitric oxide production in stromal fibroblasts, which failed to directly respond to *Mtb*^{hk} due to absence of TLR2 expression. Thus we propose that both, T cells and TipDCs regulate NOS2 production in stromal cells. Our data suggest that this mechanism is not limited to the lymphatic system. In fact, T cells and TipDCs infiltrate the heart in EAM, and NOS2 is detected in gp38-positive cardiac fibroblasts only within the inflamed myocardium. Of note, paracrine NOS2 regulation by TipDCs is not restricted to stromal cells only. Our data clearly show that *Mtb*^{hk}-activated TipDCs promote NOS2 production also in other monocyte-derived cells. Thus, *Mtb*^{hk} triggers several cellular mechanisms of NOS2 up-regulation, which consequently all negatively regulate T cell responses.

Taken together, we demonstrated that innate immune signalling, which initially triggers autoimmune responses, also activates counter-regulatory NOS2-dependent mechanisms protecting from exaggerated T cell responses. Our observation might explain the fact, that we rarely observe massive T cell responses in patients with myocarditis. Counter-regulatory mechanisms, however, might protect from fulminant myocarditis at the cost of chronic, smoldering inflammation promoting pathological remodelling and inflammatory cardiomyopathy development. Indeed, innate signalling has been recognized to promote phenotype of dilated cardiomyopathy in EAM[20], and IFN-γ is known to regulate Th2 and Th17 responses, which were

reported to modulate postinflammatory myocardial remodelling[27]. Further studies are needed to elucidate a potential role for IFN-γ and nitric oxide mediated down-regulation of heart-specific autoimmunity in the human system.

Acknowledgments: We thank Marta Bachman for outstanding technical assistance and Flow Cytometry Facility at University Zurich for excellent sorting service.

Funding Sources: The study was supported by the Swiss National Science Foundation (Grant 32003B_130771 to U.E. and 31003A_130488/1 to S.A.L.) and Swiss National Science Foundation MHV subsidy (Grant PMPDP3_129013 to G.K.). Furthermore, P.B. acknowledges support from the Swiss Heart Foundation and Olga Mayenfisch Foundation, U.E. from the Swiss Life Foundation and G.K. from the Hartmann Müller Foundation and Holcim Foundation.

Conflict of Interest Disclosures: None.

References:

1. Lv H, Havari E, Pinto S, Gottumukkala RV, Cornivelli L, Raddassi K, Matsui T, Rosenzweig A, Bronson RT, Smith R, Fletcher AL, Turley SJ, Wucherpfennig K, Kyewski B, Lipes MA. Impaired thymic tolerance to alpha-myosin directs autoimmunity to the heart in mice and humans. *J Clin Invest.* 2011;121:1561-1573.

2. Nindl V, Maier R, Ratering D, De Giuli R, Zust R, Thiel V, Scandella E, Di Padova F, Kopf M, Rudin M, Rulicke T, Ludewig B. Cooperation of Th1 and Th17 cells determines transition from autoimmune myocarditis to dilated cardiomyopathy. *Eur J Immunol.* 2012;42:2311-2321.

3. Rose NR. The adjuvant effect in infection and autoimmunity. *Clin Rev Allergy Immunol.* 2008;34:279-282.

4. Mills KH. TLR-dependent T cell activation in autoimmunity. *Nat Rev Immunol.* 2011;11:807-822.

5. Neu N, Rose NR, Beisel KW, Herskowitz A, Gurri-Glass G, Craig SW. Cardiac myosin induces myocarditis in genetically predisposed mice. *J Immunol.* 1987;139:3630-3636.

6. Eriksson U, Kurrer MO, Sonderegger I, Iezzi G, Tafuri A, Hunziker L, Suzuki S, Bachmaier K, Bingisser RM, Penninger JM, Kopf M. Activation of dendritic cells through the interleukin 1

receptor 1 is critical for the induction of autoimmune myocarditis. *J Exp Med.* 2003;197:323-331.

7. Valaperti A, Marty RR, Kania G, Germano D, Mauermann N, Dirnhofer S, Leimenstoll B, Blyszczuk P, Dong C, Mueller C, Hunziker L, Eriksson U. CD11b+ monocytes abrogate Th17 CD4+ T cell-mediated experimental autoimmune myocarditis. *J Immunol.* 2008;180:2686-2695.

8. Kania G, Blyszczuk P, Stein S, Valaperti A, Germano D, Dirnhofer S, Hunziker L, Matter CM, Eriksson U. Heart-infiltrating prominin-1+/CD133+ progenitor cells represent the cellular source of transforming growth factor beta-mediated cardiac fibrosis in experimental autoimmune myocarditis. *Circ Res.* 2009;105:462-470.

9. Blyszczuk P, Behnke S, Luscher TF, Eriksson U, Kania G. GM-CSF promotes inflammatory dendritic cell formation but does not contribute to disease progression in experimental autoimmune myocarditis. *Biochim Biophys Acta.* 2013;1833:934-944.

10. Eriksson U, Kurrer MO, Bingisser R, Eugster HP, Saremaslani P, Follath F, Marsch S, Widmer U. Lethal autoimmune myocarditis in interferon-gamma receptor-deficient mice: enhanced disease severity by impaired inducible nitric oxide synthase induction. *Circulation.* 2001;103:18-21.

11. Eriksson U, Kurrer MO, Sebald W, Brombacher F, Kopf M. Dual role of the IL-12/IFN-gamma axis in the development of autoimmune myocarditis: induction by IL-12 and protection by IFN-gamma. *J Immunol.* 2001;167:5464-5469.

12. Afanasyeva M, Wang Y, Kaya Z, Stafford EA, Dohmen KM, Sadighi Akha AA, Rose NR. Interleukin-12 receptor/STAT4 signaling is required for the development of autoimmune myocarditis in mice by an interferon-gamma-independent pathway. *Circulation.* 2001;104:3145-3151.

13. Bevan AL, Zhang H, Li Y, Archard LC. Nitric oxide and Coxsackievirus B3 myocarditis: differential expression of inducible nitric oxide synthase in mouse heart after infection with virulent or attenuated virus. *J Med Virol.* 2001;64:175-182.

14. Cuervo H, Guerrero NA, Carbajosa S, Beschin A, De Baetselier P, Girones N, Fresno M. Myeloid-derived suppressor cells infiltrate the heart in acute Trypanosoma cruzi infection. *J Immunol.* 2011;187:2656-2665.

15. Hiraoka Y, Kishimoto C, Takada H, Nakamura M, Kurokawa M, Ochiai H, Shiraki K. Nitric oxide and murine coxsackievirus B3 myocarditis: aggravation of myocarditis by inhibition of nitric oxide synthase. *J Am Coll Cardiol.* 1996;28:1610-1615.

16. Holscher C, Kohler G, Muller U, Mossmann H, Schaub GA, Brombacher F. Defective nitric oxide effector functions lead to extreme susceptibility of Trypanosoma cruzi-infected mice deficient in gamma interferon receptor or inducible nitric oxide synthase. *Infect Immun.* 1998;66:1208-1215.

17. Serbina NV, Salazar-Mather TP, Biron CA, Kuziel WA, Pamer EG. TNF/iNOS-producing dendritic cells mediate innate immune defense against bacterial infection. *Immunity.* 2003;19:59-70.

18. Serbina NV, Pamer EG. Monocyte emigration from bone marrow during bacterial infection requires signals mediated by chemokine receptor CCR2. *Nat Immunol.* 2006;7:311-317.

19. Langlet C, Tamoutounour S, Henri S, Luche H, Ardouin L, Gregoire C, Malissen B, Guilliams M. CD64 expression distinguishes monocyte-derived and conventional dendritic cells and reveals their distinct role during intramuscular immunization. *J Immunol.* 2012;188:1751-1760.

20. Blyszczuk P, Kania G, Dieterle T, Marty RR, Valaperti A, Berthonneche C, Pedrazzini T, Berger CT, Dirnhofer S, Matter CM, Penninger JM, Luscher TF, Eriksson U. Myeloid differentiation factor-88/interleukin-1 signaling controls cardiac fibrosis and heart failure progression in inflammatory dilated cardiomyopathy. *Circ Res.* 2009;105:912-920.

21. Blyszczuk P, Berthonneche C, Behnke S, Glonkler M, Moch H, Pedrazzini T, Luscher TF, Eriksson U, Kania G. Nitric oxide synthase 2 is required for conversion of pro-fibrogenic inflammatory CD133+ progenitors into F4/80+ macrophages in experimental autoimmune myocarditis. *Cardiovasc Res.* 2013;97:219-229.

22. Reifenberg K, Lehr HA, Torzewski M, Steige G, Wiese E, Kupper I, Becker C, Ott S, Nusser P, Yamamura K, Rechtsteiner G, Warger T, Pautz A, Kleinert H, Schmidt A, Pieske B, Wenzel P, Munzel T, Lohler J. Interferon-gamma induces chronic active myocarditis and cardiomyopathy in transgenic mice. *Am J Pathol.* 2007;171:463-472.

23. Fairweather D, Frisancho-Kiss S, Yusung SA, Barrett MA, Davis SE, Gatewood SJ, Njoku DB, Rose NR. Interferon-gamma protects against chronic viral myocarditis by reducing mast cell degranulation, fibrosis, and the profibrotic cytokines transforming growth factor-beta 1, interleukin-1 beta, and interleukin-4 in the heart. *Am J Pathol.* 2004;165:1883-1894.

24. Michailowsky V, Silva NM, Rocha CD, Vieira LQ, Lannes-Vieira J, Gazzinelli RT. Pivotal role of interleukin-12 and interferon-gamma axis in controlling tissue parasitism and inflammation in the heart and central nervous system during Trypanosoma cruzi infection. *Am J Pathol.* 2001;159:1723-1733.

25. Dominguez PM, Ardavin C. Differentiation and function of mouse monocyte-derived dendritic cells in steady state and inflammation. *Immunol Rev.* 2010;234:90-104.

26. King IL, Dickendesher TL, Segal BM. Circulating Ly-6C+ myeloid precursors migrate to the CNS and play a pathogenic role during autoimmune demyelinating disease. *Blood.* 2009;113:3190-3197.

27. Fairweather D, Stafford KA, Sung YK. Update on coxsackievirus B3 myocarditis. *Curr Opin Rheumatol.* 2012;24:401-407.

DOI: 10.1161/CIRCULATIONAHA.112.000434

Figure Legends:

Figure 1. IFN-γ signalling on non-lymphocytes controls EAM development. **(A,B)** Shown is the quantification of $CD45^+$ **(A)** and $CD3^+$ **(B)** immunopositive cells on heart sections of α-MyHC/CFA immunized wild-type (white) and *Ifng*$^{-/-}$ (black) mice at the indicated stages of EAM. **(C,D)** Splenic $CD4^+$ T cells from wild-type (white) and *Ifng*$^{-/-}$ (black) mice at day 21 of EAM were restimulated with α-MyHC peptide in the presence of wild-type **(c)** or *Ifngr1*$^{-/-}$ **(D)** APCs for 48h. Incorporation of [^{3}H]-thymidine indicates cell proliferation. Mean values±SD, n=3, data are representative of 3-4 independent experiments. **(E)** Wild-type ($CD45.1^+$) and *Ifngr1*$^{-/-}$ ($CD45.2^+$) splenocytes were mixed and transferred into *Rag2*$^{-/-}$ mice. After 3 weeks, the mixed chimeric mice were immunized with α-MyHC/CFA. Flow cytometry analysis of CD45.1 and CD45.2 alloantigens (right) gated on $CD3^+CD4^+$ T cells (left) shows donor cells used for injection (top) and splenocytes (middle) and heart inflammatory cells (bottom) of the mixed chimeras at day 16 of EAM. Numbers indicate percent of cells in the adjacent gates. Representative plots of 4-8 independent mice. **(F,G)** Quantification of CD45 **(F)** and CD3 **(G)** immunopositive cells on heart sections of α-MyHC/CFA immunized *Rag2*$^{-/-}$ mice reconstituted with wild-type (white diamonds) or *Ifngr1*$^{-/-}$ (black diamonds) splenocytes. **(H,I)** Quantification of CD45 **(H)** and CD3 **(I)** immunopositive cells on heart sections of α-MyHC/CFA immunized *Rag2*$^{-/-}$ (white triangles) and *Rag2*$^{-/-}$*Ifngr1*$^{-/-}$ (black triangles) mice reconstituted with wild-type splenocytes. p values computed with Student's *t*-test.

Figure 2. Heat-killed *M. tuberculosis* suppresses T cell proliferation through IFN-γR-dependent nitric oxide. **(A)** OVA-specific $CD4^+$ T cells (from DO11.10-*tg* mouse) were CFSE-labeled and

transferred to *Rag2*$^{-/-}$ and *Rag2*$^{-/-}$*Ifngr1*$^{-/-}$ mice prior treatment with IFA or CFA in the absence and presence of OVA peptide. Mice were analysed 72h later. Histograms show CFSE-dilutions of an individual representative of indicated groups of mice (n=3-4). **(B)** Proliferation index (number of divisions of dividing cells) of CFSE-labeled DO11.10-*tg* CD4$^+$ T cells (5x10^4) co-cultured with *Rag2*$^{-/-}$ (white) or *Rag2*$^{-/-}$*Ifngr1*$^{-/-}$ (black) splenocytes (2x10^5) in the presence or absence of 10 µg/mL heat-killed *M. tuberculosis* (*Mtb*^{hk}) and 2 µg/mL OVA peptide. Data are representative of 3 independent experiments, mean values±SD, n=3, *p<0.05 (Student's *t*-test). **(C-F)** *Rag2*$^{-/-}$ (white, **C,D**) and *Rag2*$^{-/-}$*Ifngr1*$^{-/-}$ (black, **E,F**) splenocytes were co-cultured with CFSE-labeled DO11.10-*tg* CD4$^+$ T cells (5x10^4) in the presence of *Mtb*^{hk} and OVA peptide without (control) or with the following inhibitors: Nω-nitro-L-arginine methyl ester hydrochloride (L-NAME, 1mM), 1-methyl-tryptophan (1-MT, 5µM) or Nω-hydroxy-nor-arginine (Nor-NOHA, 50µM). Proliferation of CFSE-labeled DO11.10-*tg* CD4$^+$ T cells **(C,E)** and nitrate levels in supernatants **(D,F)** were analyzed after 72h. Mean values±SD, *p<0.017 versus control (Student's *t*-test). **(G)** Nitrate levels in supernatants of *Rag2*$^{-/-}$ (white) or *Rag2*$^{-/-}$*Ifngr1*$^{-/-}$ (black) splenocytes and DO11.10-*tg* CD4$^+$ T cells co-cultured in the presence or absence of *Mtb*^{hk} and OVA peptide for 72h. **(H-J)** *Rag2*$^{-/-}$ (white) or *Rag2*$^{-/-}$*Ifngr1*$^{-/-}$ (black) splenocytes (2x10^5) cultivated in the presence or absence of *Mtb*^{hk} and IFN-γ. Cells were analyzed for *Nos2* mRNA **(H)** and supernatants for NOS2 **(I)** and nitrate **(J)** after 72h. Mean values±SD, *p<0.05 (Student's *t*-test), n.d. - not detected

Figure 3. NF-κB pathway controls NOS2-dependent nitric oxide production. **(A,B)** NF-κB activity measured in NF-κB reporter cells expressing TLR2 (HEK-Blue TLR2, **a**) or control (HEK-Blue Null1, **B**) unstimulated (control) and stimulated with 50 ng/mL TNFα, 1 µg/mL

Pam3CSK4, 10 μg/mL *Mtb*^{hk} or 20 ng/mL *Mtb* membrane vesicles (MV). **(C)** Representative immunofluorescence of NF-κB p65 (green) in non-stimulated (control) and stimulated (30 min) wild-type (left) and *Tlr2*$^{-/-}$ (right) bone marrow-derived macrophages. DAPI (blue) was used to stain nuclei, magnification x200. **(D,E)** Wild-type (white) and *Tlr2*$^{-/-}$ (grey) bone marrow-derived macrophages (5x10^5) were cultured in the presence (+) or absence (-) of IFN-γ and stimulated with Pam3CSK4, *Mtb*^{hk} or *Mtb* MV. Cell supernatants were analyzed for nitrate **(D)** and TNFα **(E)** after 72h. Mean values±SD, *p<0.05 (Student's *t*-test). **(F-I)** *Rag2*$^{-/-}$ splenocytes (2x10^5) were pretreated (1h) with vehicle or irreversible NF-κB inhibitor Bay 11-7082 (Bay). **(F,G)** Pretreated cells were cultured in the presence of IFN-γ without (control) or with *Mtb*^{hk} and analyzed for *Nos2* mRNA **(F)** and supernatants for nitrate **(G)** after 72h. **(H,I)** Pretreated cells were co-cultured with DO11.10-*tg* CD4$^+$ T cells in the presence of OVA peptide without (control) or with *Mtb*^{hk}. Proliferation of CFSE-labeled DO11.10-*tg* CD4$^+$ T cells **(H)** and nitrate levels in supernatants **(I)** were analyzed after 72h. Mean values±SD, *p<0.05 (Student's *t*-test)

Figure 4. *M. tuberculosis* antigens induce formation of NOS2-producing monocyte-derived dendritic cells. **(A)** Representative flow cytometry analysis of intracellular NOS2 in *Rag2*$^{-/-}$ splenocytes cultivated in the absence (control) and presence of *Mtb*^{hk} and/or IFN-γ (as indicated on top of the diagrams) for 72h. NOS2-positive cells were analyzed for CD11b and CD11c (right). Numbers indicate percent of cells in the adjacent gates. FL-2 - empty channel. Data are representative of 3 independent experiments. **(B)** Representative flow cytometry dot plots of naïve splenocytes (left) and iLN cells (right) stained with anti-CD11c and anti-CD11b antibodies. Gated cells were sorted and used for further analysis. Value in gates indicates percentage. **(C-E)** Sorted splenic CD11b^{hi}CD11c$^-$ cells (gating in **B**, 5x10^4) were cultured unstimulated (control) or

in the presence of 50 ng/mL IFN-γ, 10 μg/mL *Mtb*^{hk}, 20 ng/mL *Mtb* MV or 50 ng/mL TNFα as indicated, and were analyzed after 72h. Shown are representative dot plots of CD11b and CD11c expression and histograms of MHC class II, CD64 and intra-cellular NOS2 **(C)**. Value shows percentage of double positive cells in the adjacent gate (dot plots). Isotype controls are shown in grey (histograms). Supernatants were analyzed for nitrate **(D)** and TNFα **(E)**. Mean values±SD, n = 4, *p<0.0125 versus control (Student's *t*-test). Data are representative of 3 independent experiments. **(F,G)** CD11b^{hi}CD11c^{-} splenocytes (gating in **B**, 5x10^4 cells) were sorted from wild-type (CD45.1$^+$) and *Tlr2*$^{-/-}$ (CD45.2$^+$) mice. Cells were cultured separately **(F)** or in co-cultures **(G)** in the presence of IFN-γ and *Mtb*^{hk} for 72h. Intracellular NOS2 was analyzed by flow cytometry on CD45.1$^+$ (wild-type, left) and CD45.2$^+$ (*Tlr2*$^{-/-}$, right) gated cells. Data are representative of 3 independent experiments. Isotype controls are shown in grey.

Figure 5. Monocyte-derived dendritic cells induce and limit T cell proliferation. (**A**) Unactivated (-) or activated with IFN-γ and *Mtb*^{hk} splenocytes were cultured in the presence of OVA peptide for 24h. Next, sorted CD11b^{hi}CD11c^{-} or CD11b^{hi}CD11c^{+} cells (gating in **Fig. 4B**) were used as APCs (10^4) in co-cultures with CFSE-labeled DO11.10-*tg* CD4$^+$ T cells (5x10^4) as indicated. Representative histograms show CFSE-dilutions of DO11.10-*tg* CD4$^+$ T cells after 72h. **(B-E)** Sorted CD11b^{hi}CD11c^{-} cells (5x10^4) from the indicated mouse strains were cultured in the presence of IFN-γ and *Mtb*^{hk} for 72h and analyzed for *Nos2* mRNA **(B)** and supernatants for nitrate **(C)**. Sorted CD11b^{hi}CD11c^{-} cells (5x10^4) were co-cultured with conventional DCs (10^4) and CFSE-labeled DO11.10-*tg* CD4$^+$ T cells in the presence of *Mtb*^{hk} and OVA peptide. Proliferation index of DO11.10-*tg* CD4$^+$ T cells **(D)** and nitrite levels in supernatant **(E)** were analyzed after 72h. Data are representative of 2 independent experiments. Mean values±SD, n =

3, *p<0.017 versus wild-type (Student's *t*-test), n.a. - not analyzed. **(F-I)** Sorted splenic $CD11b^{hi}CD11c^{-}$ cells ($5x10^4$) from wild-type (white) or *Tlr2*$^{-/-}$ (black) were cultured in the presence of IFN-γ without (control) or with *Mtb*^{hk} and analyzed for *Nos2* mRNA **(F)** and supernatants for nitrate **(G)** after 72h. Sorted $CD11b^{hi}CD11c^{-}$ cells ($5x10^4$) were co-cultured with conventional DCs (10^4) and CFSE-labeled OT-II-*tg* $CD4^+$ T cells in the presence of OVA peptide without (control) or with *Mtb*^{hk}. Proliferation index of OT-II-*tg* $CD4^+$ T cells **(H)** and nitrite levels in supernatant **(I)** were analyzed after 72h. Data are representative of 2 independent experiments. Mean values±SD, n = 3-4, *p<0.05 (Student's *t*-test).

Figure 6. *M. tuberculosis* antigens fail to regulate nitric oxide production in pLN2 stromal fibroblasts. **(A)** Representative flow cytometry analysis of TLR2 in bone marrow macrophages (left) and pLN2 cells (right). Isotype controls are shown in grey. **(B)** Nuclear translocation of NF-κB p65 (green) in pLN2 cells. Cells were treated for 30 min without (control) or with 10 ng/mL IFN-γ, 50 ng/mL TNFα, 1 μg/mL Pam3CSK4, 10 μg/mL *Mtb*^{hk} or 20 ng/mL *Mtb* MV. DAPI (blue) was used to stain nuclei, magnification x200. Data are representative of 3 independent experiments. **(C,D)** pLN2 cells were cultured in the absence (control) or presence of IFN-γ (+IFN-γ) and without (white) or with TNFα (green), *Mtb*^{hk} (black) or *Mtb* MV (red) for 72h and analyzed for *Nos2* mRNA **(C)** and supernatants for nitrate **(D)**. Mean values±SD, n = 4, *p<0.017 versus controls (white, Student's *t*-test). **(E,F)** Conventional DCs and OT-II-*tg* CFSE-labeled $CD4^+$ T cells were co-cultured without (-) or with (+) pLN2 cells in the absence (control) or presence of *Mtb*^{hk} or *Mtb* MV. Proliferation index of OT-II-*tg* $CD4^+$ T cells **(E)** and nitrite levels in supernatants **(F)** are shown. Mean values±SD, n = 3, *p<0.017 versus control +pLN2 (Student's *t*-test). Data are representative of 3 independent experiments. **(G)** Sorted

$CD11b^{hi}CD11c^{-}$ splenocytes (gating in **Fig. 4B**) from *Nos2*$^{-/-}$ mice were co-cultured with pLN2 cells in the presence of IFN-γ (white) or IFN-γ and *Mtb*^{hk} (grey) for 72h and analyzed for nitrate in supernatants. Data are representative of 3 independent experiments. Mean values±SD, n = 3, *p<0.05 (Student's *t*-test).

Figure 7. Heat-killed *M. tuberculosis* in the adjuvant promotes formation of NOS2-positive monocyte-derived dendritic cells in EAM. Balb/c mice were subcutaneously immunized with α-MyHC/CFA into the right groin and with α-MyHC/IFA into the left groin **(A)** and inguinal lymph nodes (iLNs) were analyzed at day 5. **(B)** Representative immunohistochemistry of NOS2 (brown) in the indicated iLN (magnification x100). **(C)** Quantification of total $CD11b^{hi}CD11c^{+}$ cells isolated from the indicated iLN. Lines link iLNs from the same mouse. p value computed with paired *t*-test. **(D,E)** Representative flow cytometry analysis of intracellular NOS2 in $CD11b^{hi}CD11c^{+}$ cells **(D)** and in $CD45^{-}gp38^{+}$ stromal cells **(E)** from the indicated iLN. Arrows show gating strategy. Numbers indicate percent of cells in the adjacent gates. Isotype controls are shown in grey.

Figure 8. NOS2 produced by either hematopoietic or non-hematopoietic cells is sufficient to prevent exacerbated EAM. **(A,B)** Representative histology of heart sections of wild-type **(A)** and *Nos2*$^{-/-}$ **(B)** mice at day 16 of EAM. **(C,D)** Quantification of immunopositive cells for CD45 **(C)** and CD3 **(D)** antigens on heart sections of α-MyHC/CFA immunized wild-type (white) and *Nos2*$^{-/-}$ (black) mice at the indicated stages of EAM. p values computed with Student's *t*-test. **(E)** Representative flow cytometry analysis of hearts from wild-type (top) and *Nos2*$^{-/-}$ (bottom) mice at day 16 of EAM. Arrows show gating strategy. Numbers indicate percent of cells in the

DOI: 10.1161/CIRCULATIONAHA.112.000434

adjacent gates. Isotype controls are shown in grey. **(F-H)** Bone marrow chimeric mice were immunized with α-MyHC/CFA 6 weeks after lethal irradiation and bone marrow reconstitution. Shown are quantification of CD45 **(F)** and CD3 **(G)** immunopositive cells and the representative NOS2 immunohistochemistry **(H**, brown, magnification x100**)** in heart sections from the indicated bone marrow chimeras at day 16 of EAM. *p<0.05 versus *Nos2*$^{-/-}$->*Nos2*$^{-/-}$ group (ANOVA followed by Bonferroni post-hoc test).

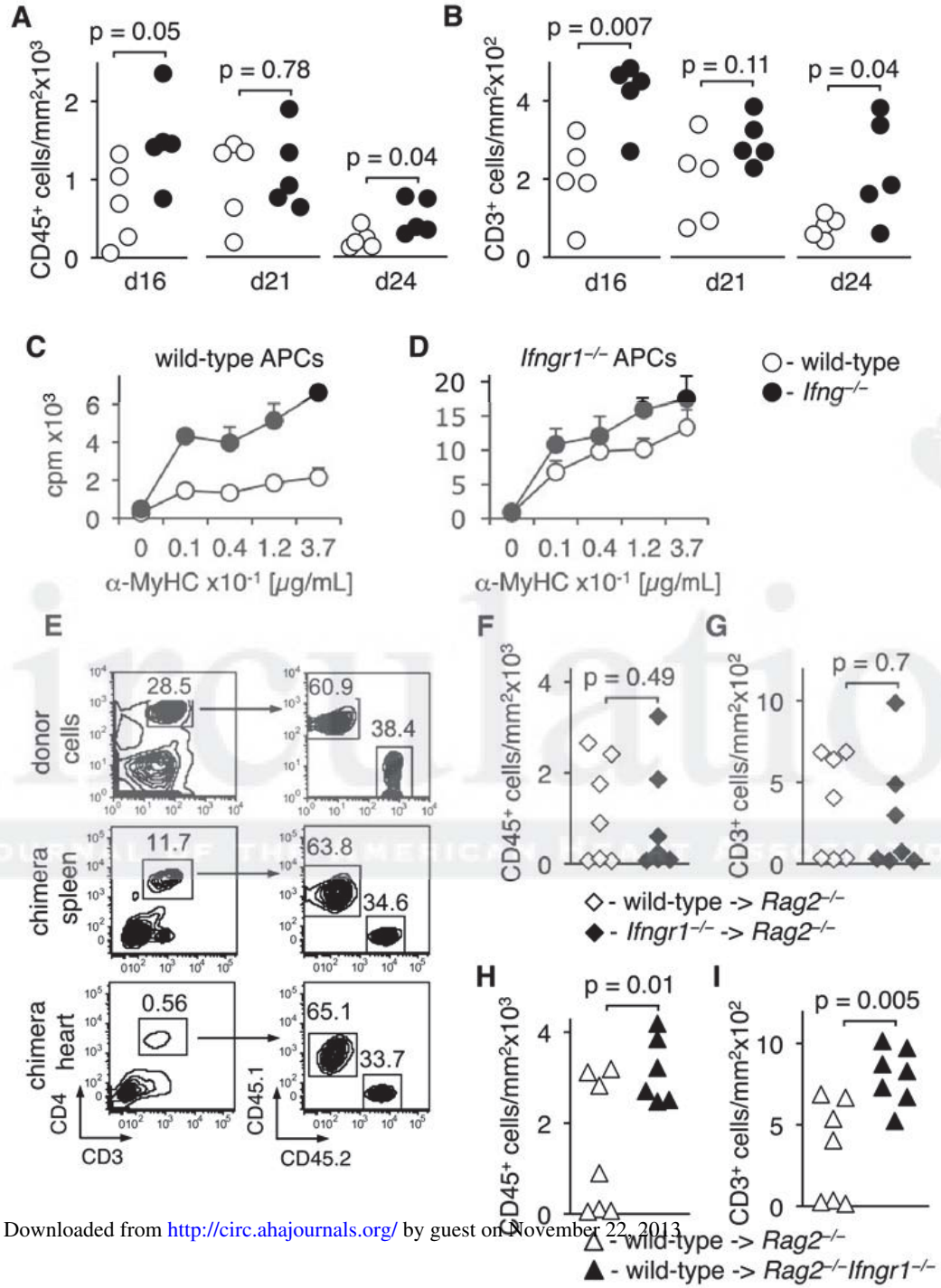

Figure 1

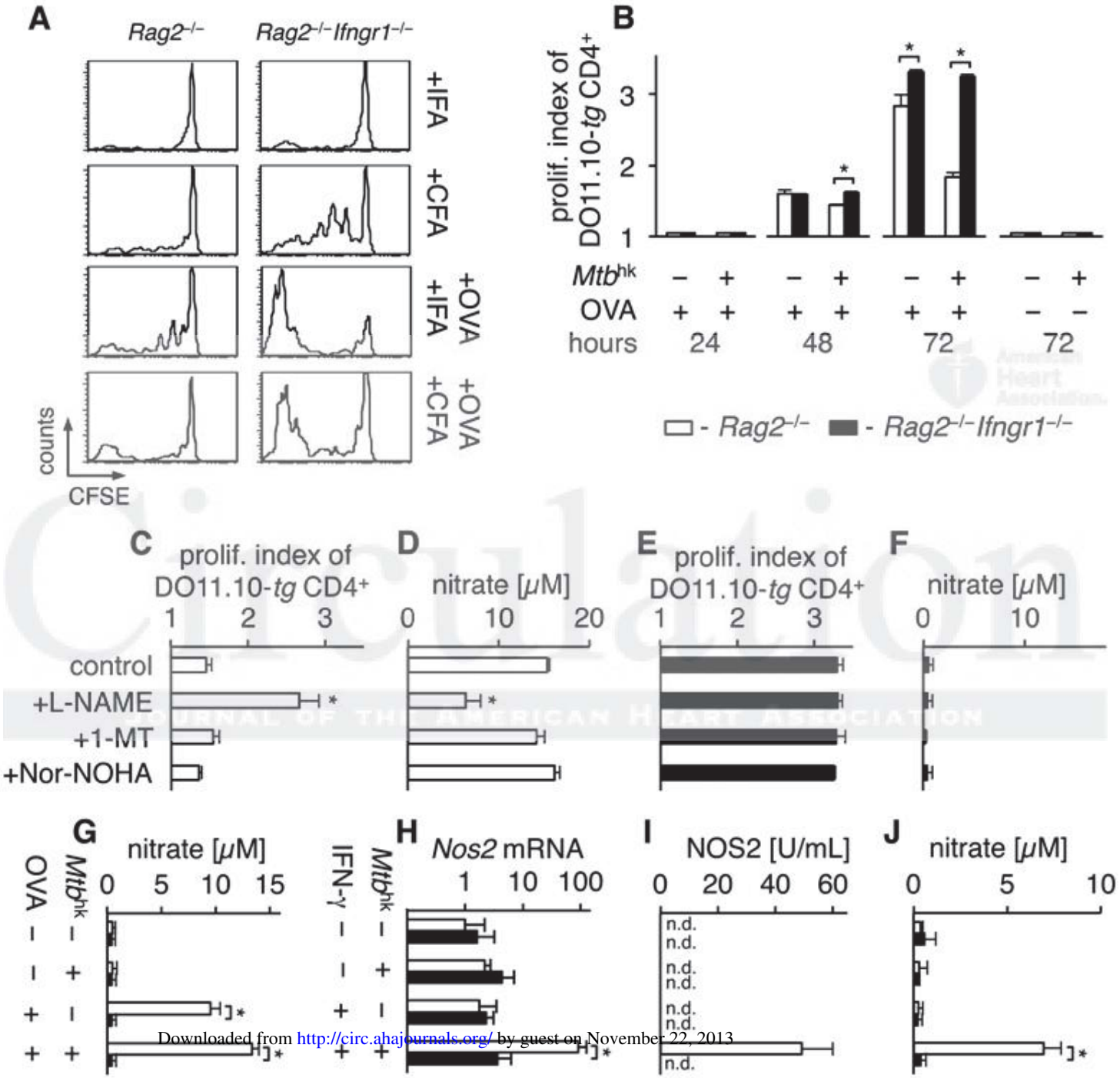

Figure 2

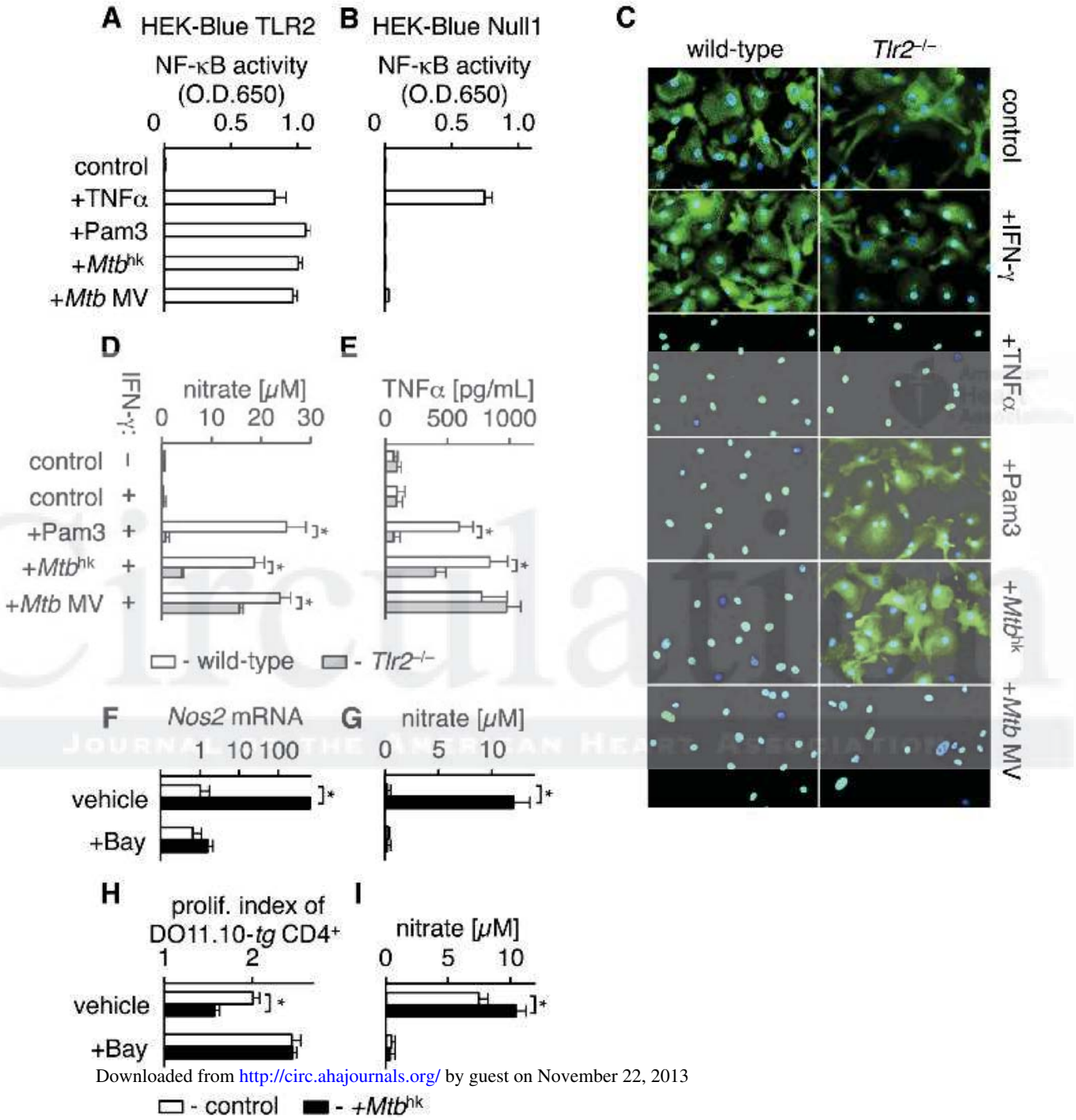

Figure 3

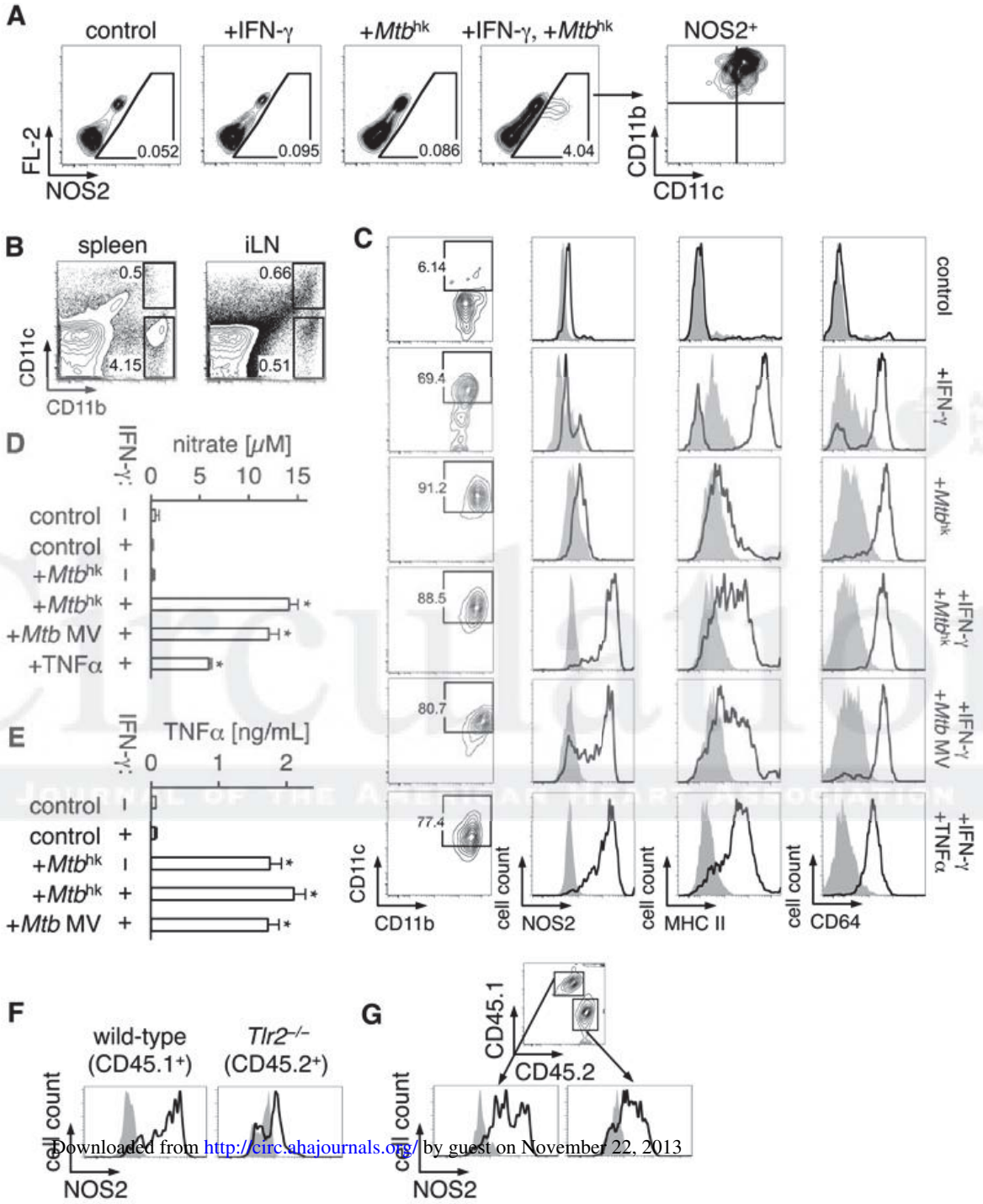

Figure 4

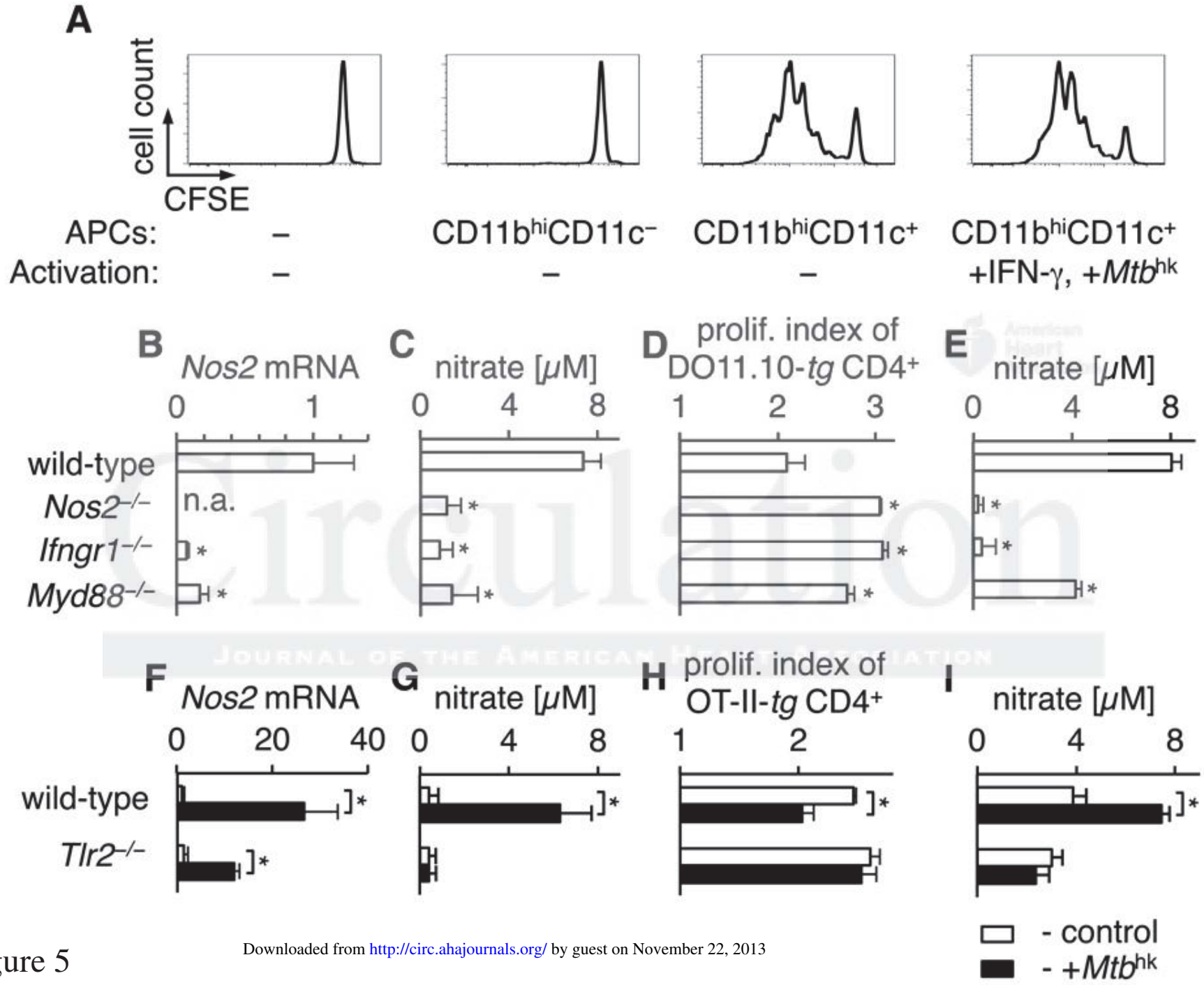

Figure 5

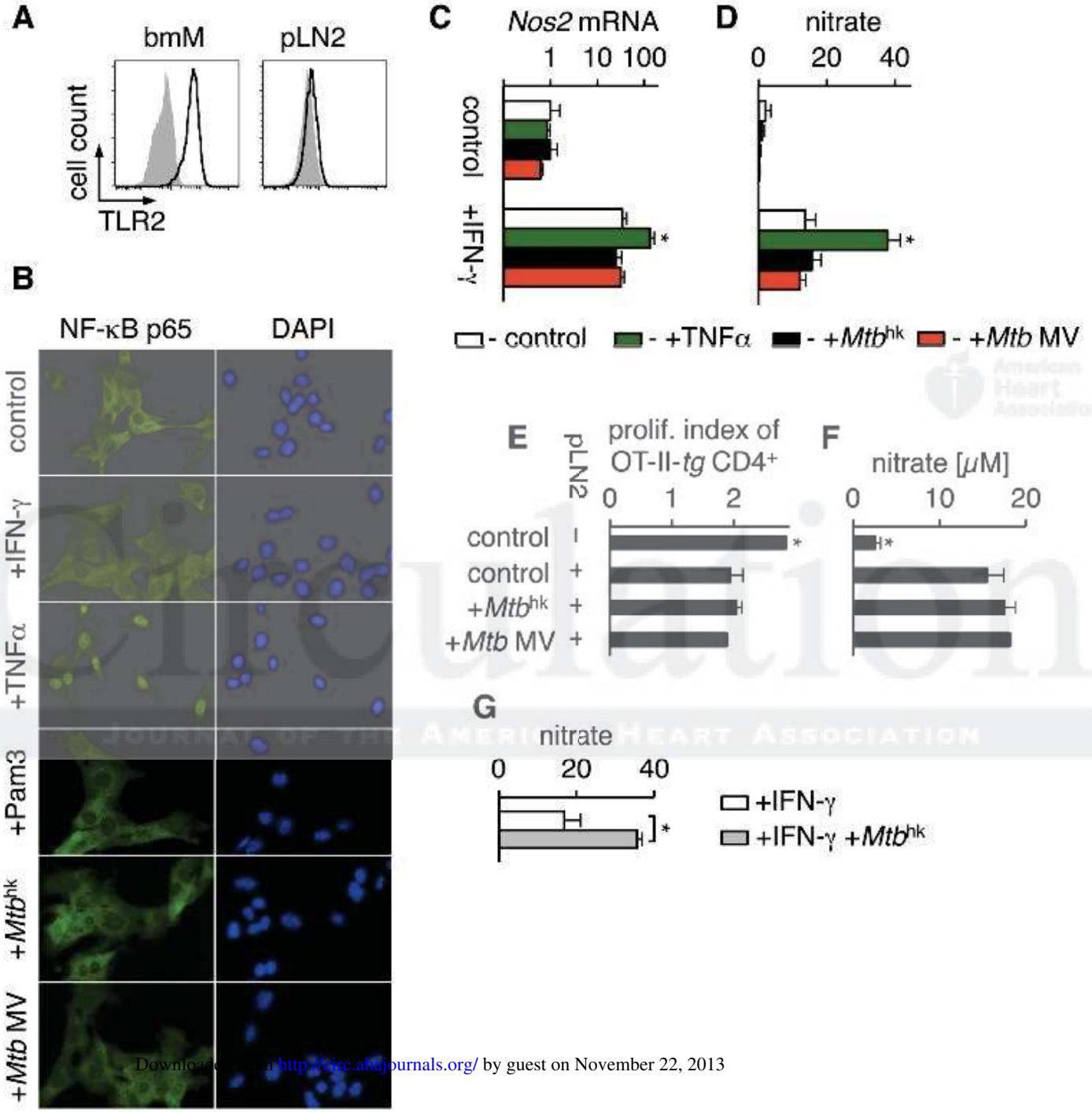

Figure 6

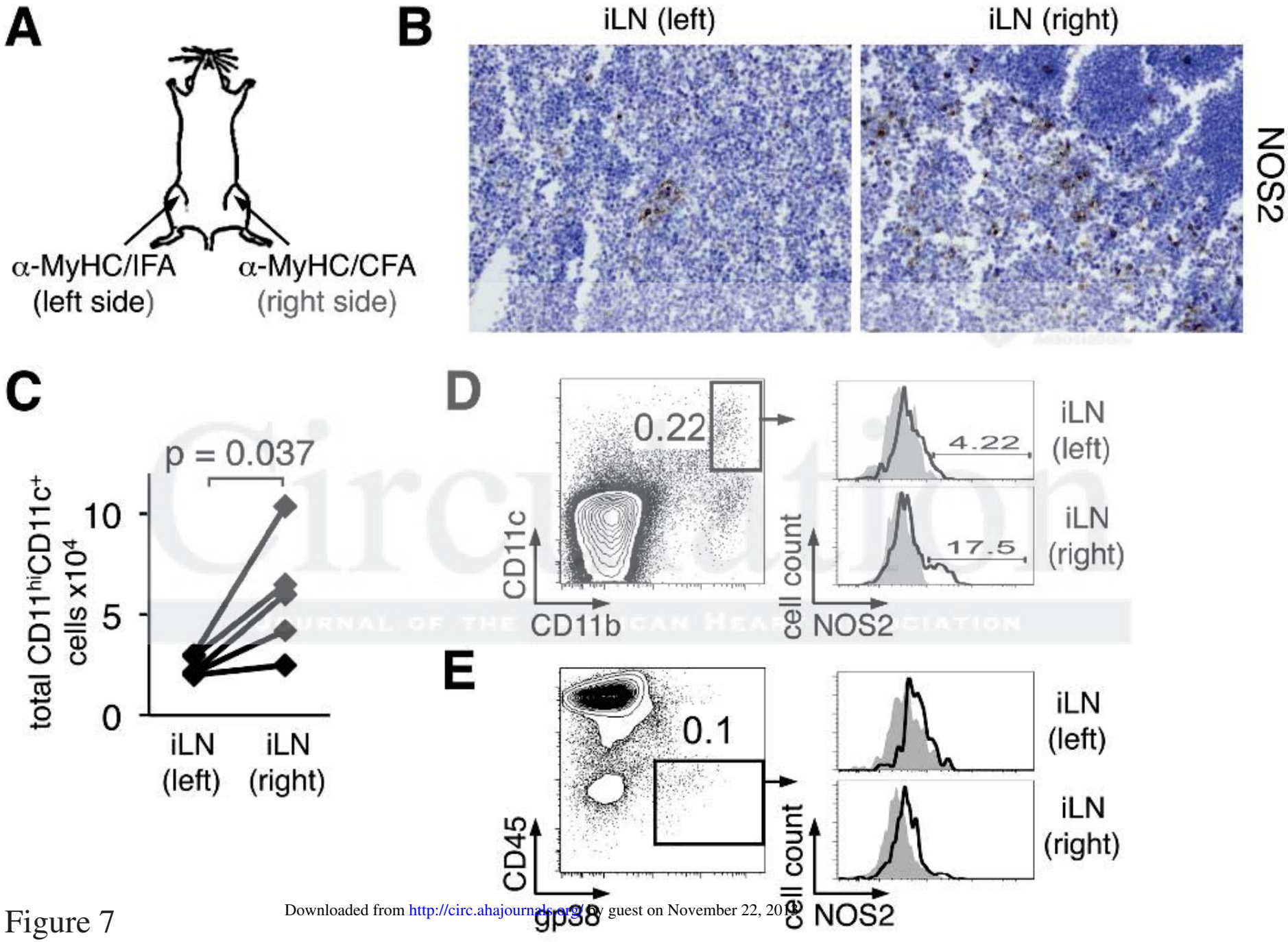

Figure 7

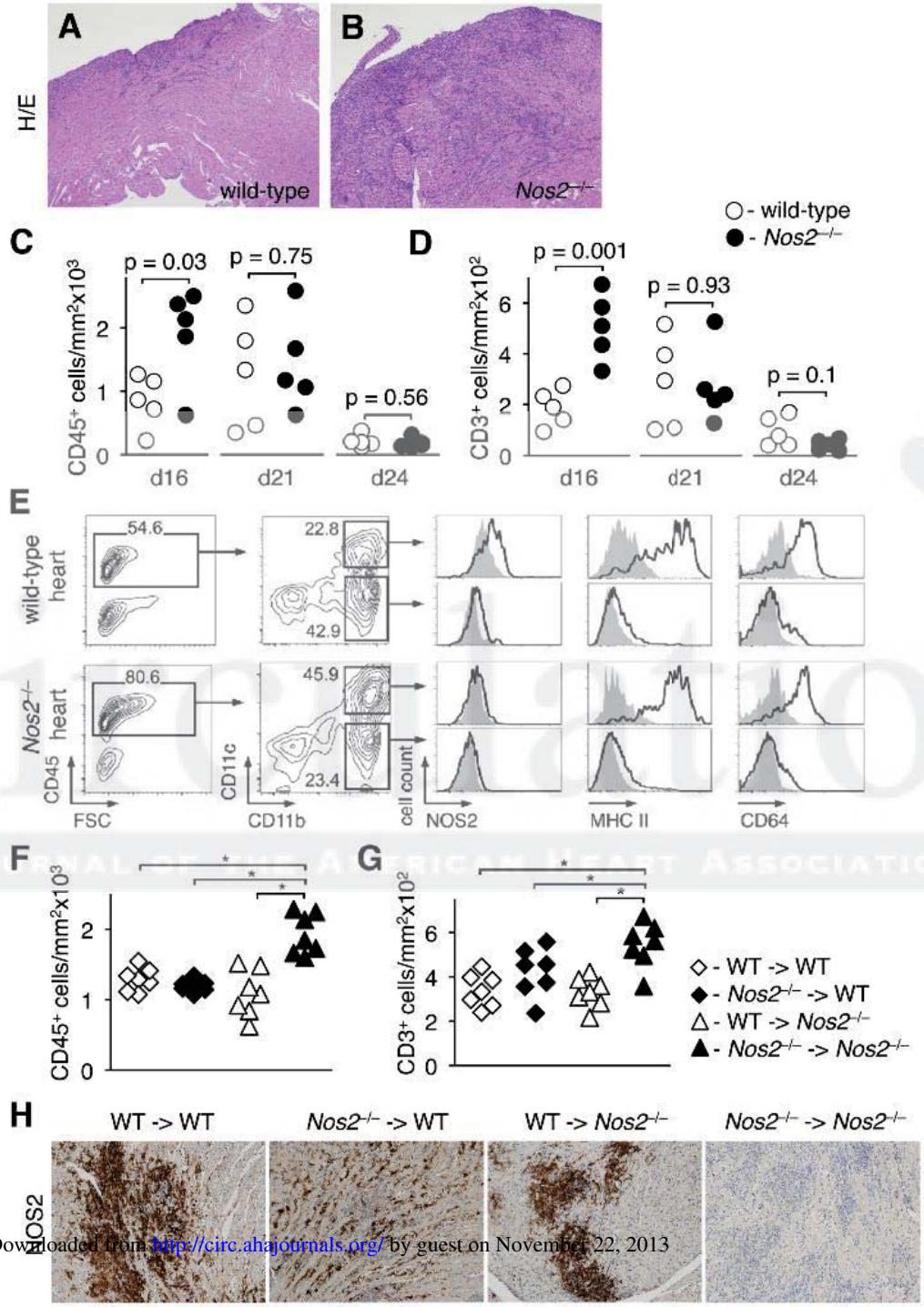

Figure 8

SUPPLEMENTAL MATERIAL

Supplemental methods

Cell culture Generations of bone marrow-derived macrophages[1] and pLN stromal cells[2] were described previously. Bone marrow-derived macrophages were stimulated at 10^6 cells/mL for 24h. Erythrocyte-lysed splenocytes were cultured at 10^6 cells/mL for 72h. FACSorted $CD11b^{hi}CD11c^{-}$ cells were cultured at $5x10^5$ cells/mL for 72h. pLN stromal cells were irradiated (1000 rad) and cultured at $5x10^4$ cells/mL for 72h. Human TLR2/NF-κB/SEAP reporter HEK293 cells HEK-Blue TLR2 and NF-kappaB/SEAP parental cell line HEK-Blue Null1 (both Invivogen) were cultured and analyzed according to manufacturer's recommendations. Cells were cultured in RPMI supplemented with 10% fetal bovine serum, penicillin/streptomycin, β-mercaptoethanol, sodium pyruvate and non-essential amino acids at 37ºC and 5% CO_2, unless otherwise indicated.

Co-cultures CD4 T cells were isolated from spleens using magnetic beads (Miltenyi Biotec) and labeled with 2.5 µM CFSE (7 min. at room temperature). $2x10^5$ *Rag2*$^{-/-}$ and *Rag2*$^{-/-}$*Ifngr1*$^{-/-}$ splenocytes were co-cultured with $5x10^4$ CFSE-labeled $CD4^+$ T cells and 2 µg/mL $OVA_{323-339}$ peptide (Anaspec) in 0.25 mL culture medium and analyzed after 72h. $5x10^4$ FACSorted $CD11b^{hi}CD11c^{-}$ cells were co-cultured with 10^4 FACSorted $CD11b^{hi}CD11c^{+}$ cells, $5x10^4$ CFSE-labeled $CD4^+$ T cells and 2 µg/mL $OVA_{323-339}$ peptide in 0.2 mL culture medium and analyzed after 72h. In the respective experiments, $5x10^4$ FACSorted $CD11b^{hi}CD11c^{-}$ cells were co-cultured with 10^4 irradiated stromal cells for 72h.

APC assay Splenocytes were cultured in the presence of 2 µg/mL $OVA_{323-339}$ peptide with or without 10 µg/mL heat-killed *M. tuberculosis* and 10 ng/mL recombinant IFN-γ for 24h and FACSorted afterward. 10^4 sorted cells were co-cultured with $5x10^4$ CFSE-labeled $CD4^+$ T cells in 0.25 mL culture medium and analyzed after 72h.

Cell treatment Cells were treated with the following reagents: 10 µg/mL heat-killed *M. tuberculosis* H37Ra (Difco), 10-100 ng/mL recombinant IFN-γ, 50 ng/mL

recombinant TNF-α (both Peprotech), 1 µg/mL Pam3CSK4, 10^8 cells/mL HKLM, 10 µg/mL Poly(I:C)-LMW, 10 µg/mL Poly(I:C)-HMW, 0.1-1 µg/mL LPS, 1 µg/mL ST-FLA, 1 µg/mL FSL-1, 1 µg/mL ssRNA, 5 µM ODN1826 (all Invivogen). Membrane vesicles produced by *M. tuberculosis* H37Ra were purified as described[3] and used at 50 ng/mL. Chemical inhibitors: 1 mM Nω-nitro-L-arginine methyl ester hydrochloride (L-NAME, Sigma), 5 µM 1-methyl-tryptophan (1-MT, Sigma) or 50 µM Nω-hydroxy-nor-arginine (Nor-NOHA, Calbiochem), 10 µM Bay 11-7082 (Sigma). Splenocytes pretreated with Bay 11-7082 for 1h at 37ºC were washed twice and resuspended in culture medium for further use.

Flow cytometry and FACS

The following antibodies were user in this study: anti-CD45 (clone 30-F11), anti-CD11c (N418), anti-CD4 (GK1.5), anti-DO11.10-TCR (KJ1-26), anti-TLR2 (mT2.7, all eBioscience), anti-CD11b (M1/70), anti-I-A/I-E (2G9), anti-CD45.1 (A20), anti-CD45.2 (104, all BD Bioscience), anti-CD3 (145-2C11), anti-CD4 (RM4-4), anti-CD64 (X54-5/7.1, all Biolegend).

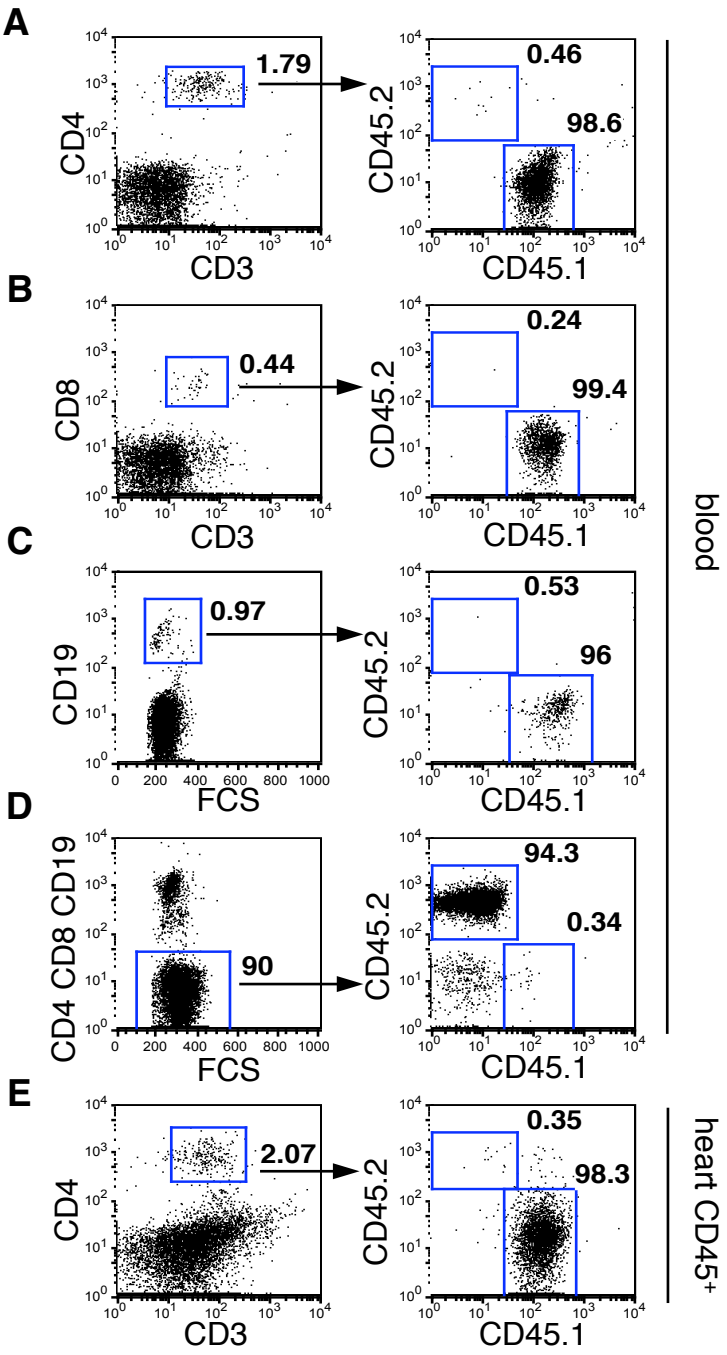

Supplementary Figure 1

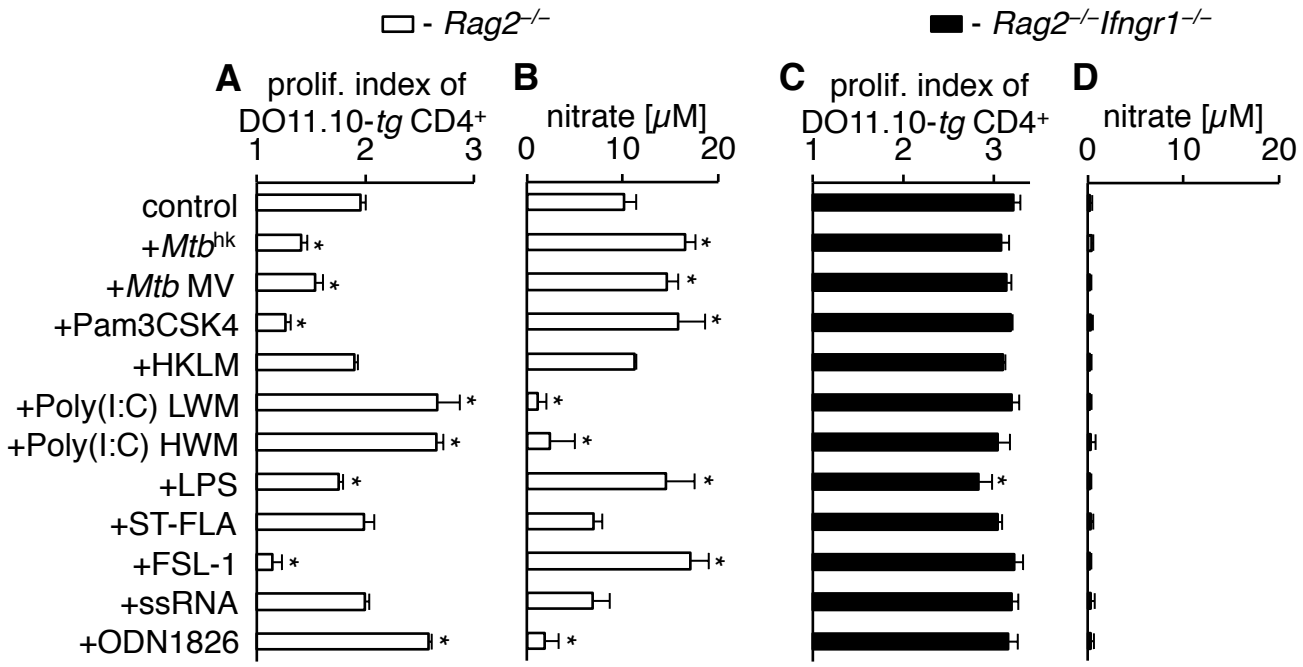

Supplementary Figure 2

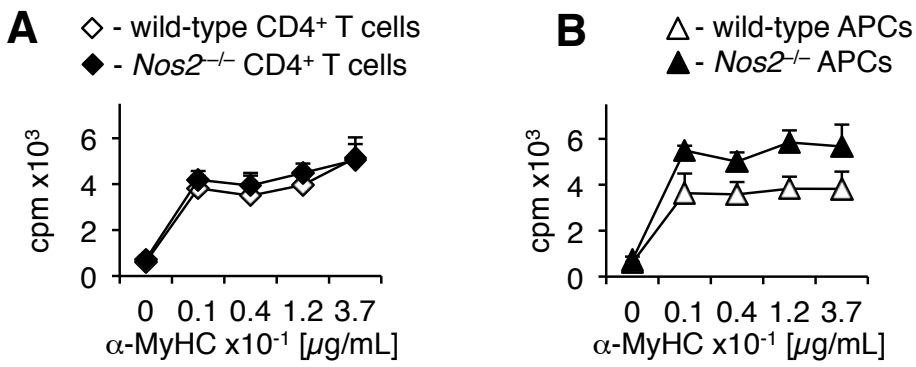

Supplementary Figure 3

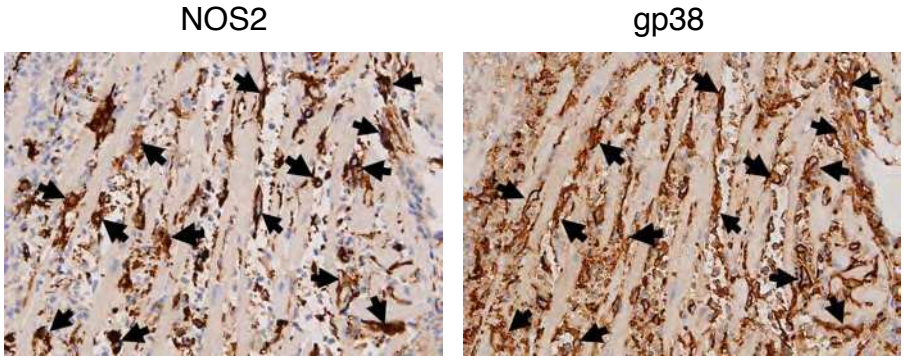

Supplementary Figure 4

Supplemental figure legends

Supplemental figure 1. Donor splenocytes reconstitute T and B cell pools in *Rag2*$^{-/-}$ mice.

The whole CD45.1^{+} splenocytes were injected into *Rag2*$^{-/-}$ (CD45.2^{+}) mice. After 3 weeks, chimeric mice were immunized with α-MyHC/CFA. Flow cytometry analysis of CD45.1 and CD45.2 alloantigens in CD4^{+} T cells **(A)**, CD8^{+} T cells **(B)**, B cells **(C)**, non-T and non-B cells **(D)** in the peripheral blood and in heart inflammatory (CD45^{+}) CD4^{+} T cells **(E)**. Arrows show gating strategy. Numbers indicate percent of cells in the adjacent gates. Representative plots of 3 mice are shown.

Supplemental figure 2. TLR agonists differentially regulate T cell proliferation and nitric oxide production.

Rag2$^{-/-}$ (white) or *Rag2*$^{-/-}$*Ifngr1*$^{-/-}$ (black) splenocytes were co-cultured with CFSE-labeled DO11.10-*tg* CD4^{+} T cells in the presence of OVA peptide without (control) or with the indicated TLR agonists. Proliferation index of CFSE-labeled DO11.10-*tg* CD4^{+} T cells **(A,C)** and nitrate levels in supernatants **(B,D)** were analyzed after 72h. Data are representative of 2-5 independent experiments, n = 3, * $p<0.05$ versus control (Student's *t*-test), n.d. - not detected

Supplemental figure 3. NOS2 production by APCs limits α-MyHC-specific proliferation in EAM

Splenocytes from wild-type (white) and *Nos2*$^{-/-}$ (black) mice at day 21 of EAM were sorted for CD4-positive T cells and CD4-negative APCs and restimulated with α-MyHC peptide. **(A)** Co-cultures of wild-type (white diamonds) or *Nos2*$^{-/-}$ (black diamonds) CD4^{+} T cells with wild-type APCs. **(B)** Co-cultures of wild-type CD4^{+} T cells with wild-type (white triangles) or *Nos2*$^{-/-}$ (black triangles) APCs. Incorporation of [^{3}H]-thymidine indicates cell proliferation. n = 6, data are representative of 2 independent experiments

Supplemental figure 4. Cardiac gp38-positive stromal cells produce NOS2 in EAM

Constitutive heart tissue sections of *Nos2*$^{-/-}$->wild-type bone marrow chimeric mouse at day 16 of EAM stained for NOS2 (left) and gp38 (right). Arrows indicate the same region of two constitutive sections. Magnification x200.

Supplemental references

1. Valaperti A, Marty RR, Kania G, Germano D, Mauermann N, Dirnhofer S, Leimenstoll B, Blyszczuk P, Dong C, Mueller C, Hunziker L, Eriksson U. CD11b+ monocytes abrogate Th17 CD4+ T cell-mediated experimental autoimmune myocarditis. *J Immunol.* 2008;180:2686-2695.

2. Siegert S, Huang HY, Yang CY, Scarpellino L, Carrie L, Essex S, Nelson PJ, Heikenwalder M, Acha-Orbea H, Buckley CD, Marsland BJ, Zehn D, Luther SA. Fibroblastic reticular cells from lymph nodes attenuate T cell expansion by producing nitric oxide. *PLoS One.* 2011;6:e27618.

3. Prados-Rosales R, Baena A, Martinez LR, Luque-Garcia J, Kalscheuer R, Veeraraghavan U, Camara C, Nosanchuk JD, Besra GS, Chen B, Jimenez J, Glatman-Freedman A, Jacobs WR, Jr., Porcelli SA, Casadevall A. Mycobacteria release active membrane vesicles that modulate immune responses in a TLR2-dependent manner in mice. *J Clin Invest.* 2011;121:1471-1483.